Distribution Category:
Nuclear Converter Reactor Fuel Cycle
Technology: Base Technology (UC-83)

ANL/RERTR/TM-11

ANL/RERTR/TM--11

DE88 003714

ARGONNE NATIONAL LABORATORY
9700 South Cass Avenue
Argonne, Illinois 60439

THE USE OF U_3Si_2 DISPERSED IN ALUMINUM IN PLATE-TYPE FUEL ELEMENTS FOR RESEARCH AND TEST REACTORS

by

J. L. Snelgrove, R. F. Domagala, G. L. Hofman, and T. C. Wiencek

Argonne National Laboratory

and

G. L. Copeland, R. W. Hobbs, and R. L. Senn

Oak Ridge National Laboratory

October 1987

The Use of U_3Si_2 Dispersed in Aluminum in Plate-Type Fuel Elements for Research and Test Reactors

J. L. Snelgrove, R. F. Domagala, G. L. Hofman, and T. C. Wiencek

Argonne National Laboratory
Argonne, Illinois 60439

and

G. L. Copeland, R. W. Hobbs, and R. L. Senn

Oak Ridge National Laboratory
Oak Ridge, Tennessee 37831

ABSTRACT

A high-density fuel based on U_3Si_2 dispersed in aluminum has been developed and tested for use in converting plate-type research and test reactors from the use of highly enriched uranium to the use of low-enriched uranium. The results of preirradiation testing and the irradiation and postirradiation examination of miniature fuel plates and full-sized fuel elements are summarized.

The swelling of the U_3Si_2 fuel particles is a linear function of the fission density in the particle to well beyond the fission density achievable in low-enriched fuels. The U_3Si_2 particle swelling rate is approximately the same as that of the commonly used UAl_x fuel particle. The presence of minor amounts of U_3Si or uranium solid solution in the fuel result in greater, but still acceptable, fuel swelling. Blister threshold temperatures are at least as high as those of currently used fuels. An exothermic reaction occurs near the aluminum melting temperature, but the measured energy releases were low enough not to substantially worsen the consequences of an accident.

It is concluded that U_3Si_2-aluminum dispersion fuel with uranium densities up to at least 4.8 Mg/m^3 is a suitable LEU fuel for typical plate-type research and test reactors.

Table of Contents

Table of Contents (Cont.)

List of Tables

List of Figures

The Use of U_3Si_2 Dispersed in Aluminum in Plate-Type Fuel Elements for Research and Test Reactors

1. INTRODUCTION

The U.S. Reduced Enrichment Research and Test Reactor (RERTR) Program was established by the U.S. Department of Energy in 1978 to provide the technical means to convert research and test reactors from the use of highly enriched uranium (HEU) fuel to the use of low-enriched uranium (LEU) fuel. In order to maintain the required excess reactivity of the reactor core, the amount of ^{235}U must be increased by 10 to 15% to overcome the additional neutron absorption of the greatly increased ^{238}U content in LEU fuel and the effects of a harder neutron spectrum. This additional ^{235}U and ^{238}U can be accommodated by increasing the uranium density of the fuel and/or by redesigning the fuel element to increase the volume fraction of fuel in the reactor core. The RERTR Program has vigorously pursued both paths with major efforts in fuel development and demonstration and in reactor analysis and design.[1]

Research and test reactor fuel elements consist of assemblies of fuel-containing plates or rods. The RERTR Program has concentrated its efforts on plate-type fuels since plate-type research and test reactors consume much more HEU than do rod-type reactors. High-density LEU rod-type fuels have been developed by GA Technologies for TRIGA reactors[2] and by Atomic Energy of Canada, Ltd.[3] Rod-type fuels will not be discussed further in this report.

The fuel plates used in the fuel elements for most research and test reactors consist of a fuel core, or "meat," in an aluminum alloy cladding. Originally, cast and wrought alloys of uranium and aluminum, consisting of UAl_3 and UAl_4 precipitates in an aluminum matrix, were used for the fuel meat. Fabrication of alloy cores with uranium densities above ~1.1 Mg U/m^3 is difficult, however, and powder metallurgical cores, with UAl_x (a combination of UAl_2, UAl_3, UAl_4, and Al phases) or U_3O_8 dispersed in aluminum, are now used in most cases. In 1978 the densest UAl_x fuel in use contained ~1.7 Mg U/m^3 in the fuel meat (~37 vol% UAl_x), and the densest U_3O_8 fuel in use contained ~1.3 Mg U/m^3 in the fuel meat (~18 vol% U_3O_8). The RERTR Program has developed and tested UAl_x and U_3O_8 dispersion fuels for LEU applications up to their practical fabrication limits--2.4 and 3.2 Mg U/m^3, respectively.

In order to minimize the need to redesign fuel elements to increase the fuel volume fraction and to make significant enrichment reductions in high-performance reactors even feasible, higher densities yet were needed. One approach, followed by the French Commissariat à l'Energie Atomique (CEA), utilized small wafers of sintered UO_2 contained in compartments of a fuel

plate produced by diffusion bonding Zircaloy frames, spacer wires, and cladding plates.[4] The 7%-enriched "caramel" fuel has performed well in OSIRIS;[5] however, fabricators of conventional plate-type fuels would have to implement a completely new fabrication process to produce caramel fuel.

The RERTR Program chose to pursue the use of high-density uranium-silicon alloys in place of UAl_x and U_3O_8 in conventional aluminum-matrix dispersion fuel in order to take advantage of the large commercial base of equipment for and experience in fabrication of such fuels. One uranium silicide compound, U_3Si_2, has been found to perform extremely well under irradiation and can provide a uranium density of at least 4.8 Mg/m^3.

The development and testing of uranium silicide fuels has been an international effort, involving other national reduced enrichment programs, several commercial fuel fabricators, and several test reactor operators. In particular, the testing of full-sized fuel elements has been performed cooperatively, with the U.S. Government providing the enriched uranium, the fuel fabricators providing the fabrication, and the U.S. Government or other governments providing the irradiations and postirradiation examinations.

Numerous results of the development and testing of uranium silicide-aluminum dispersion fuels have been published previously. The results for U_3Si_2 dispersions are summarized in this report to facilitate the preparation and review of requests to use this fuel in research and test reactors.

2. PROPERTIES OF U_3Si_2 AND OTHER URANIUM SILICIDES

2.1 Uranium Silicide Phases

As is the case for uranium aluminide, uranium silicide normally consists of a mixture of intermetallic compounds, or phases. The quantity of each phase present depends upon the composition and homogeneity of the alloy and on its heat treatment. Since, as will be discussed later, the different uranium silicide phases behave differently under irradiation, knowledge of the phases to be expected in the fuel is necessary to correctly interpret the test results and to prepare specifications. A brief discussion of this topic follows; more detail can be found in Ref. 6.

The U-Si phase diagram is shown in Fig. 1. In the region of the phase diagram between 7.3 and 10.6 wt% Si, the two phases U_3Si_2 and USi exist, at equilibrium, in the proportions shown in Fig. 2. These two phases form directly upon cooling from the liquid state. The situation is more complicated for Si contents of less than 7.3 wt% because U_3Si is formed by a peritectoid (solid state) reaction. The as-cast alloy consists of primary U_3Si_2 with a

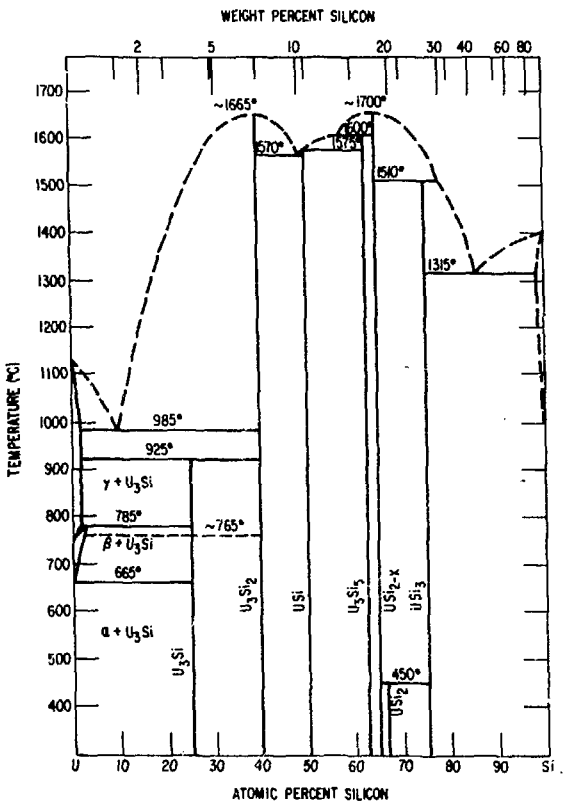

Fig. 1. The U-Si System.

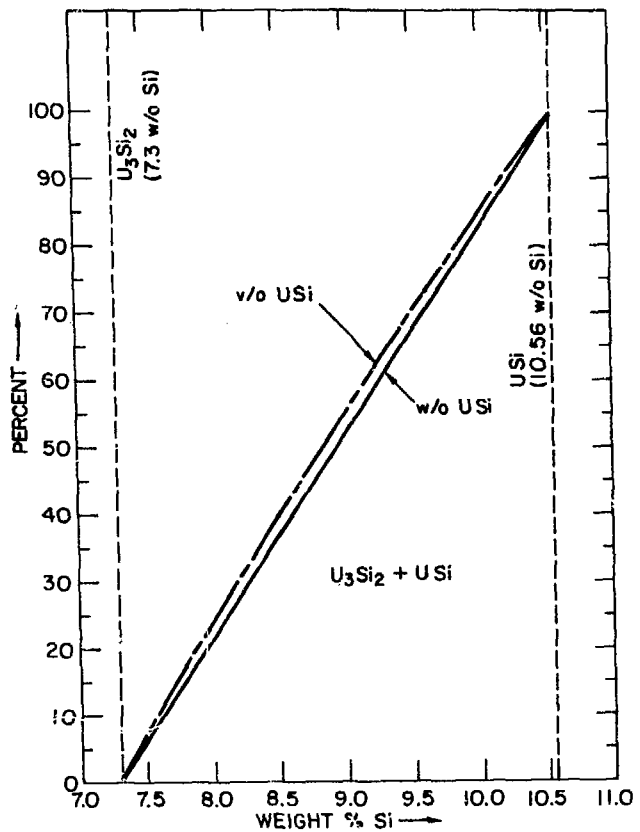

Fig. 2. Weight % (w/o) and Volume % (v/o) of USi vs. Weight % Si for Alloys at Equilibrium.

eutectic matrix of uranium solid solution (U_{ss}) and U_3Si_2. The proportions of U_3Si_2 and U_{ss} are shown in Fig. 3. Following prolonged heat treatment below the 925°C peritectoid temperature, U_{ss} reacts with U_3Si_2 to form U_3Si. Heat treatment of arc-cast ingots for 72 h at 800°C has been found to be sufficient to carry the reaction to completion. At equilibrium in the heat-treated alloy, the proportions of U_3Si and U_3Si_2 for Si contents between 3.9 and 7.3 wt% are shown in Fig. 4. Below 3.9 wt% Si the heat-treated alloy contains both U_3Si and U_{ss}.*

In practice it is essentially impossible to produce a perfectly homogeneous alloy at the exact stoichiometric composition of U_3Si_2 or to obtain equilibrium conditions. Therefore, the alloy can always be expected to contain two or more phases.† If the average composition is close to 7.3 wt%, local inhomogeneities may result in some regions of the as-cast alloy containing U_3Si_2 and USi and other regions containing U_3Si_2 and U_{ss}. If the alloy is then heat treated, the U_{ss} will be converted to U_3Si.

The practice at ANL has been to produce alloys slightly to the Si-rich side of U_3Si_2, typically 7.5 wt% Si, in order to minimize the possibility of the alloy containing measurable quantities of either U_{ss} or U_3Si. The U_3Si_2 irradiation tests discussed in this report have been obtained for fuels with Si contents ranging from ~7.2 to ~7.7 wt%. Some of the fuel was heat treated and some was used in the as-cast condition. The maximum amounts of secondary phases estimated to be present were 2 to 3 vol% of U_{ss}, 10 vol% of U_3Si, or 15 vol% of USi.

In this report and in other literature discussing uranium silicide-aluminum dispersion fuels, the convention is to use the name of the dominant phase for those alloys with average composition near that of the dominant phase. It must be remembered, however, that other minor phases will also be present and may contribute to the macroscopic behavior of the fuel.

2.2 Selected Physical and Mechanical Properties

Both U_3Si_2 and USi are brittle while U_3Si is tough and relatively soft. The measured hardness of U_3Si_2 was 742 DPH, compared to 265 DPH for U_3Si.[7]

---

*At its experimentally determined composition, 3.9 wt% Si, U_3Si actually contains 1.03 atoms of Si for every three atoms of U.

†The presence of impurities, which are not being considered here, complicates the situation further, since they may lead to the existence of still other phases.

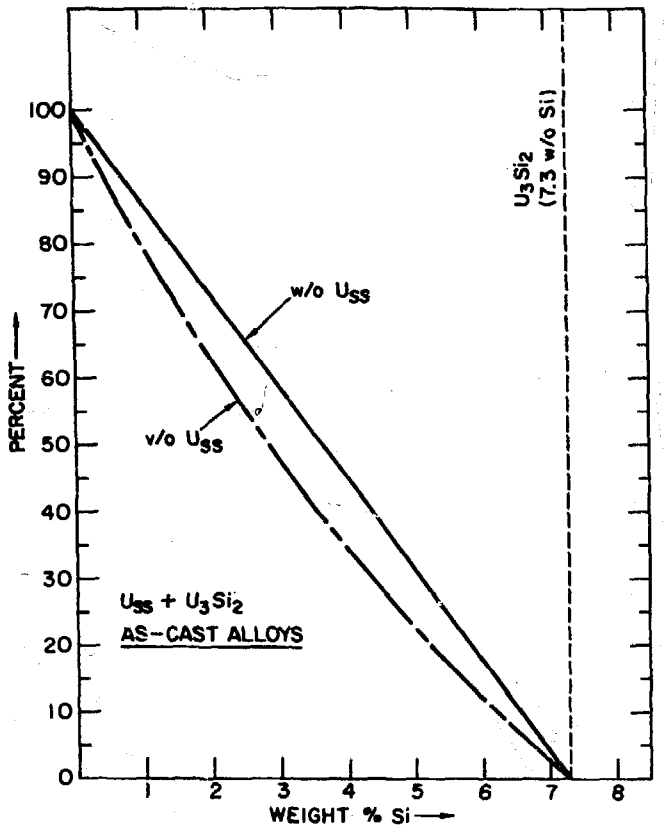

Fig. 3. Weight % (w/o) and Volume % (v/o) of Uranium Solid Solution (U_{SS}) vs. Weight % Si for As-Cast Alloys.

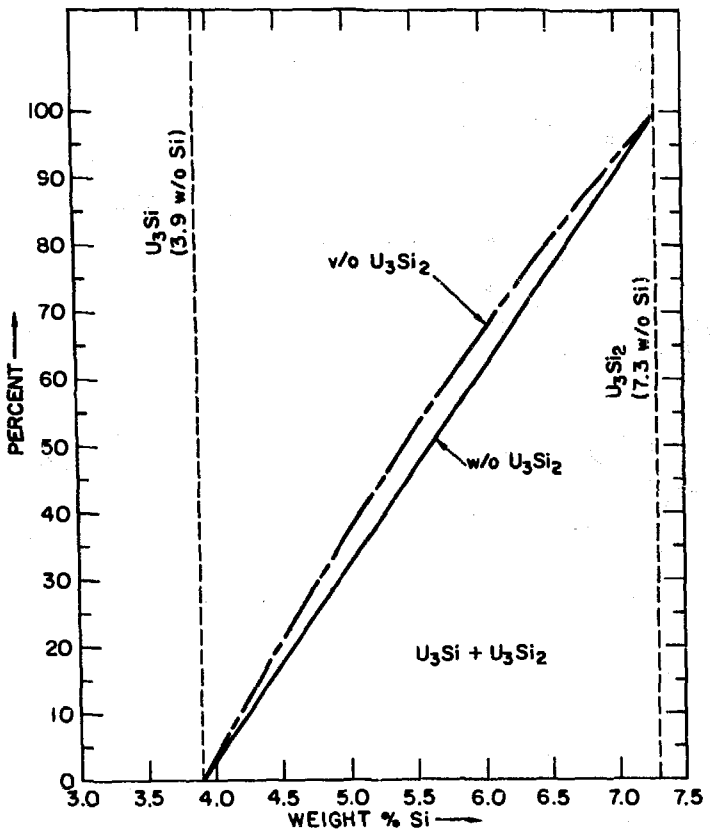

Fig. 4. Weight % (w/o) and Volume % (v/o) of U_3Si_2 vs. Weight % Si for Alloys at Equilibrium and Temperature <925°C.

The average thermal expansion coefficients of U_3Si_2 and U_3Si over the range 20 to 600°C are 15.2×10^{-6} and 15.8×10^{-6} per °C, respectively.[8]

A least squares quadratic fit of measured density vs. Si content for a series of depleted U-Si alloys with composition ranging from 4.0 to 7.5 wt% Si[7] and for USi[9] yields 12.2 and 15.4 Mg/m^3 for the densities of stoichiometric U_3Si_2 and U_3Si, respectively. For the fit the density of (depleted) USi was taken to be 10.86 Mg/m^3.[9] These densities are reduced by a negligible 0.2% for 20%-enriched uranium and by 1.1% for 93%-enriched uranium.

Both U_3Si_2 and U_3Si have a thermal conductivity of ~15 W/m·K.[8] Plots of specific heat data for stoichiometric U_3Si and for a U-Si alloy at 6.1 wt% Si are found in Ref. 10. From these data the specific heats of U_3Si_2 and U_3Si as a function of temperature (T, °C) have been derived:

$$C_p(U_3Si_2) = 199 + 0.104T \quad J/kg\cdot K \tag{1}$$

$$C_p(U_3Si) = 171 + 0.019T \quad J/kg\cdot K. \tag{2}$$

3. FUEL PLATE FABRICATION

3.1 Procedures

The procedures which have been used in fabricating U_3Si_2 fuel plates for irradiation tests are very similar to those already in use for UAl_x fuel. The procedures used at ANL to fabricate miniature fuel plates (miniplates) for irradiation testing are discussed in Ref. 11. Each of the commercial fabricators participating with the RERTR Program in the development and testing of U_3Si_2 fuel was encouraged to use its standard fabrication techniques and materials as much as was possible. A very brief general discussion of fabrication techniques follows.*

3.1.1 Fuel Powder

The uranium silicide alloys used in all of the irradiation tests were produced by melting uranium metal and elemental silicon in proper proportions in an arc furnace. The ingots were flipped and remelted from three to six times to produce a homogeneous material. Induction melting can also be used.

As discussed in Section 2.1, heat treatment (72 h at 800°C) is necessary only in those cases in which U_3Si is to be one of the end phases. In the

*A full set of procedures followed at ANL to produce miniplates is available on request from the authors.

early development work at ANL and, consequently, for the first U_3Si_2 ORR test elements produced by NUKEM* and CERCA,† the U_3Si_2 ingots were heat treated. The primary concern was that there be no U_{ss} present in the fuel plates. In later work, it was decided that heat treatment of U_3Si_2 ingots served no practical purpose, and, since it would add cost to commercial fabrication, the heat treatment step was eliminated. Hence, the fuel for all but the first four miniplates fabricated at ANL and for the ORR test elements produced by B&W** was not heat treated.

Both U_3Si_2 and USi are brittle and easily reduced to powder. In fact, the biggest concern is not to reduce the particle size too much. For the small volumes of powder needed at ANL, the U_3Si_2 was comminuted by hand using a steel mortar and pestle. Jaw crushers and/or hammer mills or ball mills were used by the commercial fabricators. Particle sizes ranged from <40 or <44 μm (fines), depending on whether metric or U.S. standard sieves were used, to 150 μm. The amount of fines in the irradiation test specimens ranged from 15 to 40 wt%. It should be noted that because of the brittle nature of U_3Si_2 and because of the high volume loading of fuel in high-density fuels, many of the larger fuel particles are broken during rolling, effectively increasing the number of fines. Uranium silicide is pyrophoric, and care must be taken when working with the powder in air. All fabricators conducted comminution in a glovebox with a neutral (N_2 or Ar) atmosphere. Average compositions and impurities of U_3Si_2 powders used to fabricate miniature plates and full-sized plates for irradiation testing are listed in Table I.

3.1.2 Fuel Plates

Fabrication of fuel plates followed the same procedures which had been established for UAl_x and U_3O_8 dispersion fuels. Fuel powder and aluminum powder were mixed in the desired proportions and formed under pressure into a powder-metallurgical compact. The compact was placed in the cavity of a "picture" frame, and cover plates to form the top and bottom cladding were welded in place to form a rolling billet. The billets were first hot rolled and then cold rolled to produce a plate of proper thickness. After hot rolling, a one-hour anneal at approximately the rolling temperature was conducted to test for the generation of blisters, indicating faulty bonding

---

*NUKEM GmbH, Hanau, Fed. Rep. of Germany.

†Compagnie pour l'Etude et la Réalisation de Combustibles Atomiques, Romans-sur-Isere, France.

**Babcock and Wilcox Company, Lynchburg, Virginia, U.S.A.

Table I. Reported Average U_3Si_2 Powder Compositions and Impurities

		Fabricator		
Major Constituent, wt%	ANL	B&W	CERCA	NUKEM
U	92.3	91.8 (91.2-92.3)	92.1	---
Si	7.5	7.4 (7.2- 7.7)	---	7.3
Impurity, ppm				
Al	26	4	---	400
B	---	5	<10	0.9
C	270	607	337	400
Cd	---	<0.5	<10	<5
Co	---	---	---	<5
Cu	---	7	---	96
Fe	96	6	---	550
H	6	---	13	---
Li	---	---	<5	<5
N	90	---	1672	---
Ni	---	5	---	---
O	429	806	1290	---
Zn	---	<2	---	<10

between cover and frame or between cover and fuel meat. Following shearing or machining to final size, the homogeneity of the uranium in the fuel meat was checked, either by real-time x-ray attenuation scanning or by densitometry of an x-radiograph. Full-sized plates for fuel elements were also inspected ultrasonically for areas of nonbond.

3.2 Special Considerations for High-Density U_3Si_2 Dispersion Fuel

Most of the fuel plates fabricated for irradiation testing contained between 40 and 50 vol% of fuel in the fuel meat, considerably in excess of the loadings of HEU dispersion fuels. Accordingly, special consideration must be given to certain fabrication procedures and/or specifications in order to achieve cost-effective yields of acceptable plates. The most important of these are briefly discussed below.

3.2.1 Dogbone

As the volume of fuel in the core increases, the core gets stronger. When the core is stronger than the frame and covers, the rolling process leaves the ends of the core thicker than the middle. A longitudinal cross section of the long, narrow fuel core with thickened ends resembles a bone, hence the name. A dogbone has two undesirable consequences: reduced cladding thickness and increased areal uranium density (the amount of uranium beneath a unit area of plate surface). The latter may result in excessively high surface heat fluxes during irradiation and be cause for rejection of the plate.

Two methods have been employed to reduce or eliminate "dogboning." If allowed by the specifications, a stronger aluminum alloy can be used for the frame and, possibly, the covers to more nearly match the strength of the fuel core. Of course, it is the strength at the rolling temperature (425 to 500°C) which is important. If the strength of the fuel core still exceeds the strength of available aluminum alloys, the ends of the compact can be tapered to compensate for the thickening at the ends of the rolled fuel core. Both methods have been successfully employed in producing high-density U_3Si_2 fuel plates for irradiation testing.

3.2.2 Minimum Cladding Thickness

As the volume loading of fuel particles increases so does the probability that fuel particles will come in contact with one another during rolling and that some will be projected into the cladding. Since the particle distribution in a dispersion fuel core is random, one cannot predict the location and depth of the penetrating particles.

Requirements for minimum cladding thickness in most specifications for HEU fuel plates date from the time of alloy cores. Once a proper set of rolling parameters had been determined for a fuel plate with an alloy core, the process was very repeatable. Core and cladding thickness could be reliably determined by examining a few metallographic sections of a few fuel plates. Unless a sophisticated and expensive device which can nondestructively measure the cladding thickness over single fuel particles is available, it is impossible to determine the actual minimum cladding thickness of a dispersion fuel plate. A statistical basis can be established for estimating minimum cladding thickness from the distribution of measured minima observed in metallographic sections of typical fuel plates.[12] Such a basis can be used to set acceptance criteria for the number of particles observed to penetrate to within a given distance of the cladding surface. One must always accept, however, the possibility that the cladding over some particles may be thinner than the stated minimum.

If a dogbone exists, there is a high probability that the point of minimum cladding exists in the dogbone region. Therefore, reducing the dogbone should increase the minimum cladding thickness. A reduction in the maximum allowed fuel particle size should decrease the penetration distance into the cladding, thereby increasing the minimum cladding thickness.

The minimum allowable cladding thickness for miniplates irradiated in the ORR was 0.20 mm. The minimum cladding thickness for full-sized fuel plates for use in test fuel elements was specified to be 0.25 mm; however, in some instances fuel plates were accepted from a batch exhibiting slightly smaller minima. No detrimental effects attributable to thin cladding were observed during testing.

3.2.3 Stray Fuel Particles

Another consequence of increased fuel loading is an increased number of fuel particles at the surface of the compact. Some of these exposed particles can be dislodged during assembly of the rolling billet or during rolling and deposited between the frame and covers--regions of the fuel plate which are supposed to be fuel free. The occurrence of stray fuel particles can be detected by examination of properly exposed x-radiographs, where the stray particles are seen as "white spots." Stray fuel particles are sources of both heat and fission products during irradiation. Unless the concentration of fuel particles is large, however, heat generation is small and of no practical consequence. Hence, the main concern is that the fuel particles not be in locations where they might become exposed to the coolant.

The occurrence of stray fuel particles can be minimized by use of adequate compacting pressure to lock most surface particles into the compact and by careful assembly of the rolling billet. NUKEM reports that the problem of stray particles can be completely eliminated by coating the compact with a thin layer of aluminum.[13,14]

Many full-sized fuel plates which should have been rejected according to the specifications were accepted on a case-by-case basis for the irradiation test elements. In some cases stray particles very near the edges or ends of a fuel plate were removed by filing.

3.2.4 Surface Oxidation of Compact

At temperatures above 177°C U_3Si_2 reacts readily with oxygen.[15-17] Since hot rolling temperatures range between 425 and 500°C, substantial oxidation of fuel particles at the surface of the compact may occur if adequate precautions are not taken to prevent air from freely entering the rolling billet during the initial heating. Recent evidence from postirradiation examinations indicates that blistering during a postirradiation anneal initiates at the sites of oxidized fuel.

4. PROPERTIES OF UNIRRADIATED U_3Si_2 DISPERSION FUEL

4.1 Fuel Meat Porosity

Porosity remaining after fabrication of dispersion fuel meat provides space to accommodate the initial swelling of the fuel particles under irradiation. The amount of as-fabricated porosity increases significantly as the volume loading of fuel increases because it becomes more difficult for the matrix aluminum to flow completely around all fuel particles, especially those in contact with one another.[18] Data obtained at ANL from measurements on U_3Si_2 miniplates are plotted in Fig. 5. These data are fit well by the cubic function

$$V_P = 0.072V_F - 0.275V_F^2 + 1.32V_F^3, \qquad (3)$$

where V_P and V_F are volume fractions of porosity and fuel in the meat, respectively.

Other parameters also have an important effect on the amount of as-fabricated porosity, although individual contributions have not been isolated. For example, consider the nominally identical U_3Si_2 elements fabricated by B&W, CERCA, and NUKEM for irradiation testing in the ORR. The porosity content of the fuel cores produced by a given fabricator remained virtually

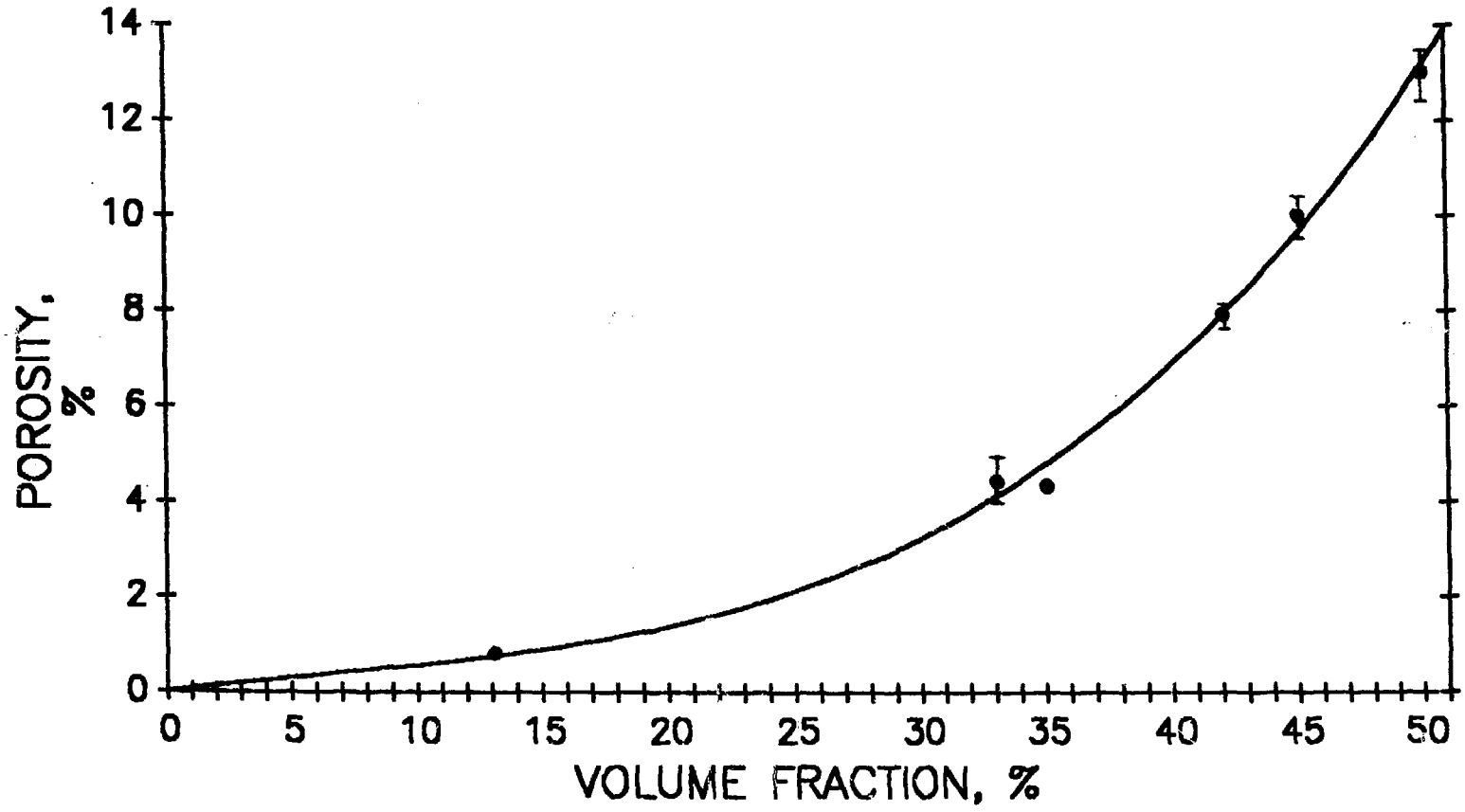

Fig. 5. Percent Porosity as a Function of the Volume Percent Fuel.

constant, but there was a variation from fabricator to fabricator: 4 vol% for CERCA, 7 to 8 vol% for NUKEM, and 9 to 10 vol% for B&W. Differences in material or fabrication parameters which might have contributed to the different amounts of porosity include: (1) strength of the aluminum alloy used for frames and covers--the CERCA alloy was by far the strongest while the B&W alloy was the weakest; (2) the rolling temperature--425°C for CERCA and NUKEM and ~500°C for B&W; (3) the amount of fines in the U_3Si_2 powder--40 wt% for CERCA and 17-18 wt% for NUKEM and B&W; (4) the rolling schedule, especially the amount of cold reduction; and (5) the relationship between the size of the compact and the size of the cavity in the frame.

Differences in the as-fabricated porosity in fuel plates will manifest themselves as differences in swelling of the plates during irradiation. Since much less constraint to swelling is offered in the thickness direction than in the length and width directions of plates, effectively all of the swelling results in a thickness increase. Early in the irradiation the plates will actually become thinner as irradiation-enhanced sintering occurs. Net swelling begins when the fuel particles have swelled enough to fill the pores. Under the same irradiation conditions, a difference of 6 vol% in as-fabricated porosity translates to a difference of 6% of the meat thickness in the final thickness of the plate. This value, ~30 to 45 μm for typical fuel meat thicknesses, is much less than the tolerances normally allowed for cooling channel thickness. Therefore, it is not expected that the normal variation of as-fabricated porosity among fabricators will have any safety implications.

4.2 Heat Capacity

The heat capacity of the fuel meat is the sum of the heat capacities of the fuel and the aluminum of the matrix. The heat capacity of U_3Si_2 is given by Eq. (1) and the heat capacity of aluminum as a function of its temperature (T, °C) is given by[19]

$$C_p(Al) = 892 + 0.46T \quad J/kg \cdot K. \tag{4}$$

The volumetric heat capacity of the fuel meat with LEU is

$$C_p(U_3Si_2\text{-}Al) = 0.0122V_F C_p(U_3Si_2) + 0.0027(1 - V_F - V_P)C_p(Al) \ MJ/m^3 \cdot K. \tag{5}$$

Using the pore volume given by Eq. (3), it is seen that the heat capacity of the fuel meat at room temperature decreases from 2.44 to 2.13 $MJ/m^3 \cdot K$ as the fuel volume fraction increases from 0 to 0.5. The decrease is primarily a result of the increase in porosity as the fuel volume fraction increases, since the volumetric heat capacities of aluminum and U_3Si_2 are very similar.

4.3 Thermal Conductivity

Values of thermal conductivities of the fuel meat in unirradiated U_3Si_2 dispersion fuel plates, measured at 60°C, are listed in Table II and plotted in Fig. 6.[20] Most of the samples were cut from miniature fuel plates produced at ANL for use in out-of-pile studies. Two samples came from a full-sized plate from a lot of plates fabricated by CERCA for the ORR test elements. The porosities of these miniature plates follow the trend discussed in Section 4.1 but are somewhat larger, owing, presumably, to the different shape of the fuel zone than in the miniplates fabricated for irradiation testing (cylindrical rather than rectangular compacts were used).

It is seen that the thermal conductivity decreases rapidly as the volume fraction of fuel plus porosity increases (and the volume fraction of matrix aluminum decreases), owing to the ~14 times larger thermal conductivity of aluminum than U_3Si_2. For very low volume loadings of fuel, it would be expected that the thermal conductivity of the dispersion would be proportional to the amount of aluminum present, since the aluminum matrix should provide a continuous thermal path. Indeed, this is the case for sample CS148. At higher volume fractions of fuel plus void, however, the aluminum ceases to be the continuous phase, and the thermal conductivity decreases more rapidly than does the volume fraction of aluminum. At very high loadings the aluminum ceases to play a significant role, and the thermal conductivity approaches that of the fuel. It may even become lower than that of the fuel alone because of poor thermal contact between fuel particles. The microstructure of the meat, specifically the distribution of the voids, can significantly affect the thermal conductivity. It appears that thin planar regions in which voids are associated with fractured fuel particles are responsible for the large difference in thermal conductivity exhibited by the CERCA samples and sample CS143. The larger void content of the CS samples than measured in the miniplates fabricated for irradiation testing or in full-sized plates most likely indicates the presence of more of such planar void regions. Therefore, it is believed that the thermal conductivity curve in Fig. 6 represents essentially a lower limit for the thermal conductivities of full-sized fuel plates.

The data for U_3Si_2 dispersions are virtually indistinguishable from those obtained in the same series of measurements for U_3Si dispersions. They are also quite similar to data obtained in other measurements of thermal conductivities of UAl_x dispersions[21] and U_3O_8 dispersions.[22] The U_3O_8 data fall somewhat below the U_3Si_2 data, possibly because the friable nature of U_3O_8 leads to the formation of more planar void regions than are present in U_3Si_2 fuel.

Table II. Thermal Conductivities of U_3Si_2-Aluminum Dispersions

Sample Identification	Fraction of Fuel -325M Mesh, wt%	Fuel Volume[1] Fraction, %	Porosity,[2] vol%	Thermal Conductivity of Dispersion at 60°C, W/m•K	Temperature Coefficient, $W/m \cdot K^2$
CS148	15	13.7	1.9	181	0.148
CS106	15	32.3	6.0	78	0.029
CS140	0	39.4	9.2	40	0.014
CS141	15	37.0	9.3	48	5×10^{-4}
CS142	25	39.1	9.5	40	0.017
CERCA #1	41.5	46.4	4.0	59	0.161
CERCA #2	41.5	46.4	4.0	59	0.076
CS143	15	46.4	15.4	13.9	0.010

[1]Determined on the thermal conductivity specimens using a radiographic technique.
[2]Average value for the roll-bonded fuel plate.

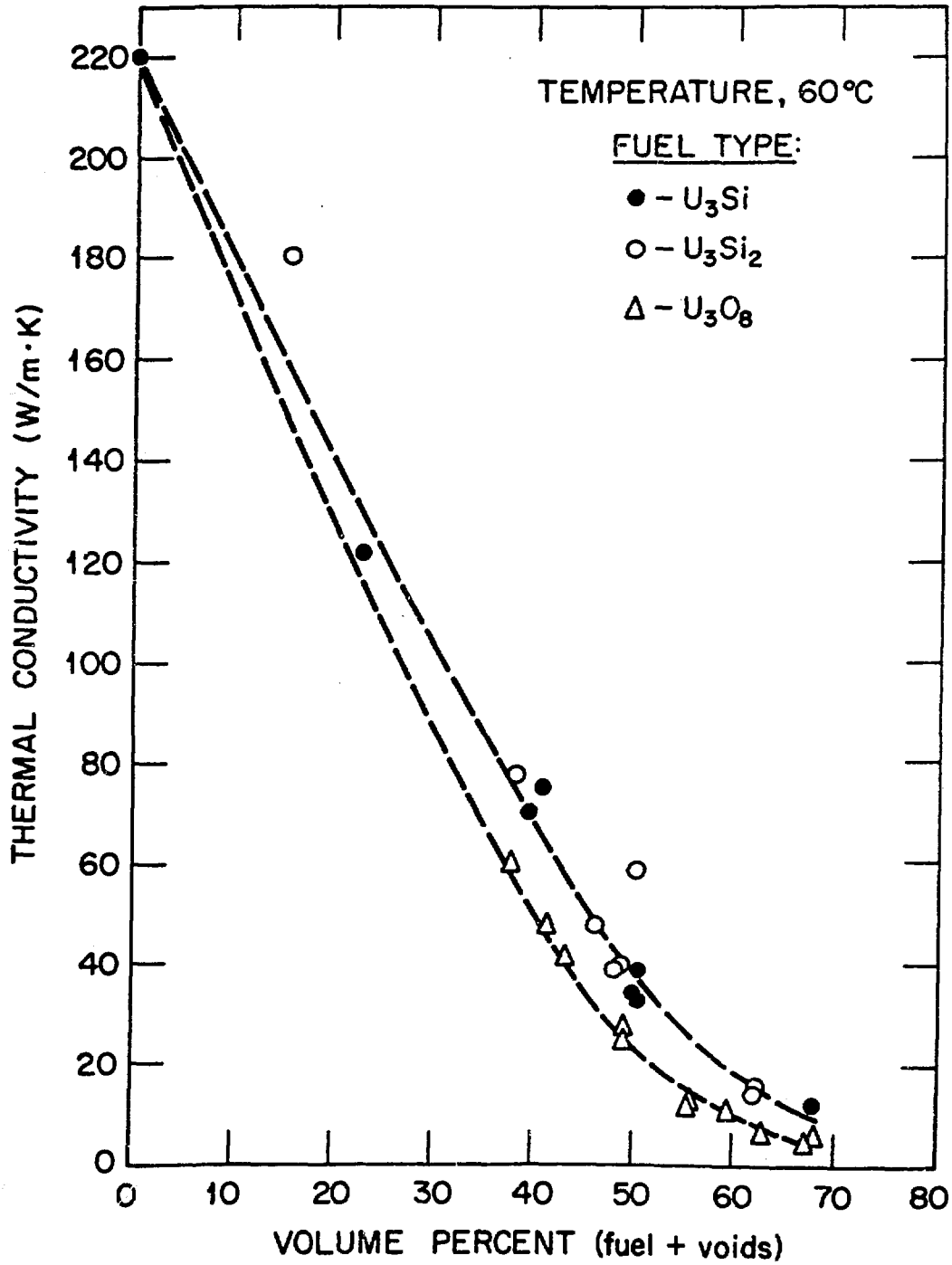

Fig. 6. Thermal Conductivities of Uranium Silicide- and U_3O_8-Aluminum Dispersion Fuels as a Function of Volume Fraction of Fuel Plus Voids (Porosity).

Even though this section properly deals with unirradiated fuel, some considerations will be set forth on how the thermal conductivity might change as the fuel is irradiated (no known data exist). Little change is expected either for very low or for very high fuel volume fractions. In the former case the thermal conductivity is essentially proportional to the amount of aluminum present in the matrix, which is effectively unchanged by the swelling fuel particles. In the latter case the thermal conductivity is much lower, approximately that of the fuel and would not be expected to change appreciably. For intermediate loadings, however, the thermal conductivity is quite sensitive to the amount of aluminum in the matrix and to the microstructure of the fuel meat. During the time that swelling fuel particles cause a reduction in the amount of as-fabricated porosity, the thermal conductivity might increase slightly, especially if planar void regions are eliminated. When the porosity has been eliminated, usually after medium burnup, irradiation-enhanced creep of the matrix aluminum toward the cladding is induced by pressure from swelling fuel particles, reducing the amount of aluminum in the matrix. This should result in a gradual decrease in thermal conductivity. As fission gas bubbles form in the fuel particles at high burnup, the conductivity might be even further reduced.

4.4 Compatibility of U_3Si_2 and Aluminum

Knowledge of the degree of compatibility of the fuel and cladding is important for any fuel system. Above about 600°C U_3Si_2 reacts rather rapidly with Al, as discussed in Section 4.5. At or below rolling temperatures (425 to 500°C), this reaction is very slow. No reaction zone surrounding the U_3Si_2 particles can be seen in optical micrographs of unirradiated fuel. Phase equilibria studies[9] indicate that the reaction product is $U(Al,Si)_3$, a phase based on UAl_3 wherein some of the Al atoms have been replaced by Si atoms in the crystal lattice.

Long-term thermal anneals of U_3Si_2 dispersions have been performed to study the compatibility of U_3Si_2 and Al.[15,16,23] In the work at ANL miniature fuel plates were fabricated by standard procedures using cylindrical compacts. Plates were annealed at 400 ± 5°C for incremental times up to 1981 hours. The plates were periodically withdrawn from the furnace, measured for volume increase, and returned to the furnace for additional annealing. The results for both 32- and 45-vol% fuel loadings are shown in Fig. 7. For comparison, data for U_3Si fuel are also shown.

The growth of uranium silicide dispersions during thermal anneals appears to be a two-step process:[23] First, the uranium silicide reacts with the aluminum of the matrix and cladding to form a less-dense product, $U(Al,Si)_3$. The early stages of swelling are due to this phenomenon. Then, as a result of

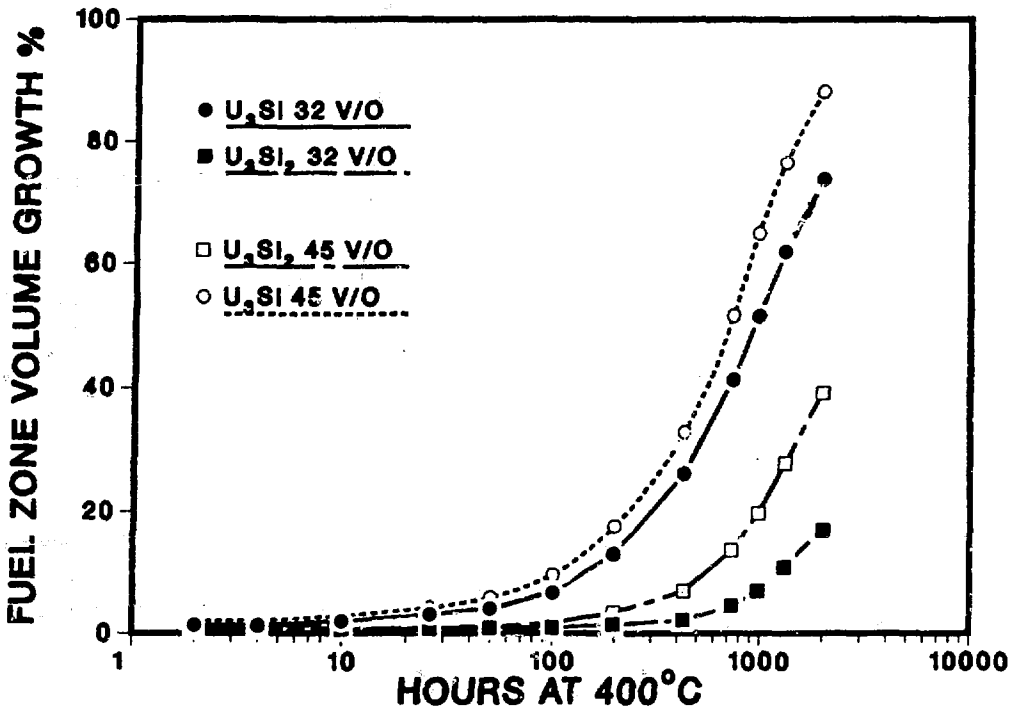

Fig. 7. Volume Percent Growth in the Fuel Zone for Uranium Silicide Fuels at 400°C.

the reaction, hydrogen, contained as an impurity in the reacting materials, is released as a gas into the pores of the meat. The strength of the fuel meat decreases as the reaction proceeds, and the pores become connected. When the internal pressure of the hydrogen exceeds the external pressure on the cladding, the cladding begins to creep and, finally, the plate "pillows".

The reaction noted above is diffusion controlled and, therefore, exponentially dependent on temperature. The rates of reaction at temperatures of 300°C or less have been demonstrated to be very low.[11] Since, as will be discussed later, there appears to be little reaction between U_3Si_2 and Al during irradiation, the mechanism of hydrogen release discussed here should not affect the swelling of U_3Si_2 dispersion fuel during irradiation at temperatures below 300°C. All evidence from irradiated plates supports this conclusion.

4.5 Exothermic Energy Releases

Early work on uranium silicide-aluminum dispersions suggested that a rapid exothermic reaction between uranium silicide and aluminum occurs at ~620°C.[24] Measurements, using differential thermal analysis (DTA) techniques, have been performed at ANL to determine the temperature regime and enthalpies of these reactions.[25] Results of similar measurements have also been reported by others.[17,26] Samples for the measurements were punched from miniature fuel plates fabricated using cylindrical compacts. Results of the DTA measurements are given in Table III, which includes values for U_3Si and U_3O_8[27] for comparison. Typical thermograms are shown in Fig. 8. The large negative ΔT is the aluminum melting endotherm. This endotherm occurs over an extended temperature range because the solidus point of the Al 6061 cladding is 582°C and the liquidus point is 652°C. The exothermic uranium silicide-aluminum reaction results in the reversal of the ΔT trace at ~640°C. Upon cooling and reheating, very little additional reaction was detected. The net effect for fuel loadings up to ~5 Mg U/m^3 was always an endotherm. For samples at 45 vol% U_3Si in the fuel zone (~6.6 Mg U/m^3), the net effect for the first heating was a very slight exotherm. No event (either exothermic or endothermic) was detected between temperatures of 660 and 1300°C.

Complete reaction of all fuel with aluminum should result in the release of the same amount of energy per unit mass of fuel for each sample tested. Insensitivity of the DTA technique to slow energy releases may be responsible for the different values determined for the different fuel loadings. The data indicated that sufficient aluminum was available in the matrix to complete the reaction in the lower-loaded U_3Si_2 samples but not in the higher-loaded U_3Si_2 samples or in the U_3Si samples. Since the reaction is diffusion controlled and since the cladding aluminum had to move larger distances to participate in

Table III. Energy Released from the Exothermic Reaction of Uranium Silicide or U_3O_8 with Aluminum in Fuel Plates

Fuel Type	Volume Loading, vol%	Reaction Energy, kJ/kg	Onset Temperature, °C
U_3Si_2	32	349 ± 44	590
U_3Si_2	45	304 ± 18	590
U_3Si	32	486 ± 54	580
U_3Si	45	379 ± 13	590
U_3O_8	44[a]	243 ± 126	890
U_3O_8	44[a]	71 ± 18	900

[a]Different cladding-to-meat-thickness ratios. Data from Ref. 27.

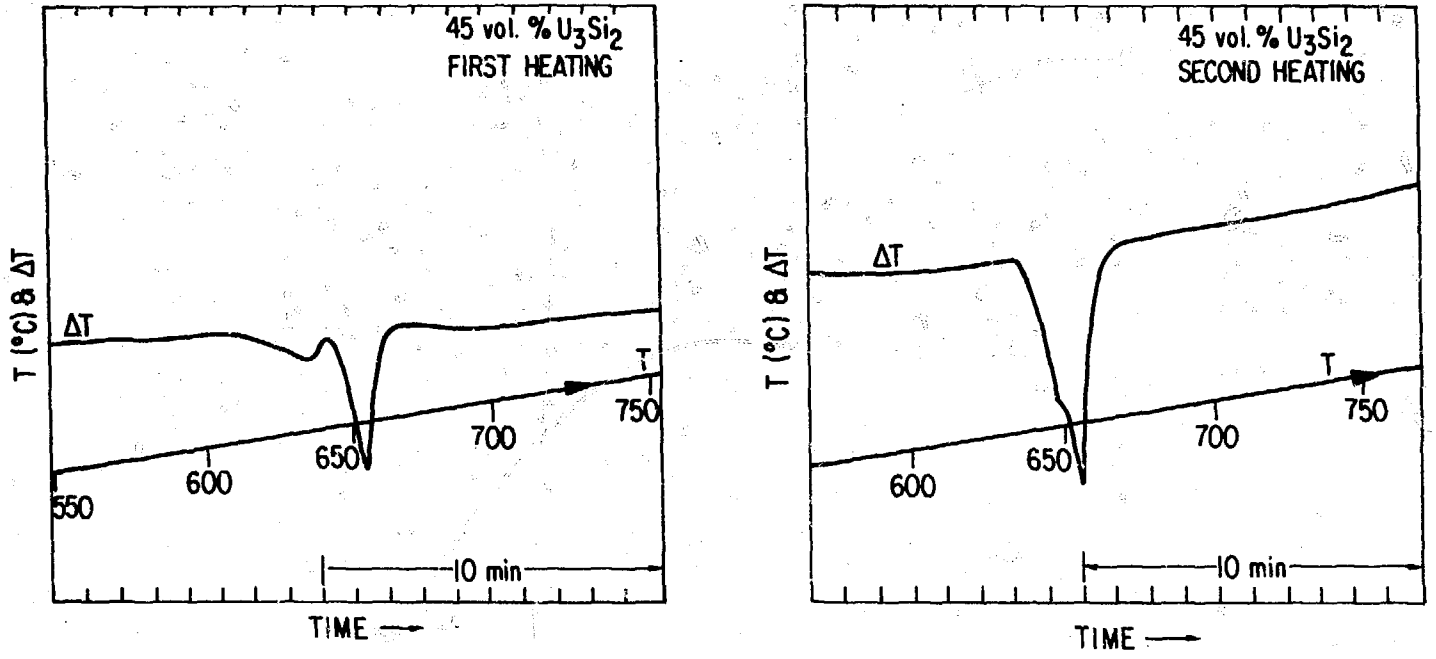

Fig. 8. Thermograms Obtained During Differential Thermal Analysis of U_3Si_2-Al Fuel Samples.

the reaction, it is possible that part of the reaction occurred too slowly to be detected by the DTA technique. If such were the case, the true reaction energy would have to be determined by extrapolation of the measured data to low volume loadings of fuel. For the U_3Si_2 fuel the extrapolated value should not be very much larger than the value for the 32-vol% case since sufficient aluminum was available in the matrix to complete the reaction.

As evident in Fig. 8, the reaction in dispersion fuel meat occurs over a period of minutes. A similar exothermic reaction in U_3O_8 dispersion fuel plates has been referred as a "thermite" reaction because of large reported energy releases.[28] More recent work[27] has shown that that reaction occurs much more slowly in fuel plates, consistent with the results for uranium silicide dispersion fuel plates. The relative slowness of the exothermic reaction means that the amount of energy supplied by the reaction will be small compared to the energy supplied by the heat source responsible for raising the temperature of the fuel plate to the reaction onset temperature. For example, an LEU fuel element containing 240 g of ^{235}U will contain ~1.3 kg of U_3Si_2, and ~450 kJ would be released by the reaction of all of the fuel in the element. That same element in a typical 2-MW reactor would produce between 50 and 100 kW, taking only 4.5 to 9 s to produce 450 kJ. After shutdown, decay heat would typically be of the order of 1% of the operating power, requiring 450 to 900 s to produce 450 kJ. Therefore, whether the initiating event were to be a flow blockage at full power or a loss of coolant, it is seen that over the course of the event and its aftermath, the contribution of the exothermic reaction is relatively small. It should also be noted that significant energy release from the exothermic reaction occurs only at temperatures above the solidus temperatures of commonly used cladding alloys; therefore, the exothermic reaction itself will not cause loss of cladding integrity.

4.6 Corrosion Behavior

A test of the corrosion resistance of U_3Si_2 dispersion fuel has been performed[11] by drilling a 3.25-mm (0.128-in.)-diam hole completely through the cladding and fuel meat of a miniplate and boiling the plate in distilled water for 168 h. The plate was withdrawn periodically during the test for weighing and examination. No radioactivity was detected in the water, nor was loose radioactivity present on the plate after the test. The plate darkened during the test, but no other changes were noted. It is concluded that the solubility in water at temperatures up to 100°C of U_3Si_2 dispersed in aluminum is negligibly small.

It should be noted that the cladding alloys used in all of the fuel tests and anticipated to be used in production fuel elements are the same alloys

which have been used in research and test reactors for many years. The corrosion behavior of these alloys is well established.

5. IRRADIATION BEHAVIOR OF U_3Si_2 DISPERSION FUEL

5.1 Irradiation Testing

The irradiation testing of fuels being developed by the RERTR Program has followed a two-stage process. First, miniplates were irradiated to determine the basic irradiation behavior of the candidate fuel. Following the miniplate irradiations, full-sized elements of a successful candidate fuel were irradiated to confirm the expected behavior of the fuel when fabricated and irradiated under typical conditions. In many instances fabrication of the elements began before complete results were available from the miniplates, in order to compress the development and testing schedule. Therefore, the test element specifications did not always reflect all that was ultimately to be learned from the miniplates. As will be seen, the resulting variety of as-fabricated properties greatly increased the value of the tests.

5.1.1 Test Samples

5.1.1.1 Miniplates

The miniature fuel plates for irradiation testing were 114 mm long by 50 mm wide and either 1.27 mm or 1.52 mm thick. The fuel meat could be up to 109 mm long by 46 mm wide. The thickness of the fuel meat was a parameter in some of the tests; its maximum was limited by the 0.20-mm minimum cladding requirement. The fuel meat and plate thicknesses were typical of those anticipated to be used in reactor conversions. The width and length of the miniplates were chosen to be sufficient to provide protypical conditions with regard to constraint of the fuel meat by the cladding and frame, i.e., the fuel meat length and width were very much greater than its thickness. The miniplate specifications[29] required that the cladding of the finished miniplate be in the O-temper condition to assure uniformity of cladding constraint conditions among miniplates produced by different fabricators. As testing progressed, it was decided that cladding temper did not play a major factor in miniplate performance, and this requirement was abondoned in order to more nearly simulate the conditions of commercially produced full-sized plates.

Miniplate irradiation testing, conducted in the Oak Ridge Research Reactor (ORR), proceeded in two phases: the screening of primary candidate fuels followed by more extensive tests of those performing acceptably. In the first series of irradiations, conducted between July 1980 and June 1983, four

U_3Si_2 and 18 U_3Si miniplates were irradiated. The second series of irradiations, conducted between March 1984 and January 1987, included ten USi, 35 U_3Si_2, and 34 U_3Si miniplates. Some plates contained fuel produced with 40%-enriched and with 93%-enriched uranium in order to establish failure thresholds and with depleted uranium in order to determine the effects of fast neutrons, as opposed to fission fragments, on the fuel. Postirradiation examinations of a number of miniplates have been completed, and the results will be discussed in Section 5.2.

5.1.1.2 Full-Sized Elements

Six full-sized U_3Si_2 fuel elements irradiated in the ORR[30] and one irradiated in the SILOE reactor at the Centre d'Etudes Nucléaires de Grenoble (CEN-G) in France in cooperation with the French CEA[31] have provided irradiation performance data under typical reactor conditions. Prior to testing a full element, CEN-G irradiated four full-sized plates, in lieu of miniplates, in SILOE. They have also irradiated four full-sized plates and a full-sized element containing U_3Si fuel.* Many more U_3Si_2 elements have been irradiated as part of a whole-core demonstration in the ORR (see Section 5.3). The ORR elements were fabricated by B&W, CERCA, and NUKEM, and the SILOE elements and plates were fabricated by CERCA. Each fabricator used its normal materials and fabrication practices, with minor modifications necessitated by the new fuel type.

The fuel elements for the ORR and SILOE were essentially identical geometrically to their standard HEU elements. The SILOE elements were assembled in such a manner that two plates were removable for interim thickness measurements. Specifications for the elements followed very closely their HEU counterparts. The nominal uranium loading in the fuel meat of the ORR elements was 4.75 Mg/m^3; the as-fabricated loadings ranged between 4.6 and 5.2 Mg/m^3. The SILOE element contained 5.2 Mg U/m^3. The ORR elements contained 19 curved plates, and the SILOE element contained 23 flat plates.

---

*Tests of U_3Si_2 elements are underway in the R2 reactor at Studsvik, Sweden, and U_3Si_2 elements are currently being fabricated for tests in the High Flux Reactor at Petten, The Netherlands. These irradiations will provide data on fuel elements containing plates with 0.76-mm-thick fuel meat and, consequently, with much higher total ^{235}U contents. These tests are not considered necessary for general qualification of U_3Si_2 fuel, however. Additional U_3Si_2 elements have been irradiated in other reactors (DR 3 in Denmark, FRG-2 in Germany, and SAPHIR in Switzerland) without the involvement of the RERTR Program, as part of the conversion studies for those reactors.

5.1.2 Reactors and Test Conditions

As stated in the previous section, irradiations of U_3Si_2 miniplates, full-sized plates, and full-sized elements have been carried out in two medium-power materials testing reactors, the ORR and SILOE. The ORR and SILOE normally operate at powers of 30 and 35 MW, respectively. Power densities in the fuel meat are similar in these reactors. In the ORR the pH and electrical resistivity of the primary coolant ranged between 5.0 and 6.3 and 0.7×10^4 and 2.5×10^4 Ω·m, respectively, during the irradiations.

The miniature fuel plates were irradiated in five stacked modules assembled in an irradiation device which could be loaded into any of the normal fuel positions of the ORR.[29] When assembled, the irradiation device resembled an ORR element with narrow fuel plates. The miniplates were irradiated in relatively high-flux positions in the core. At the end of each irradiation cycle, typically two to three weeks in length, channel gap thicknesses were measured with an ultrasonic probe to detect the onset of rapid swelling of any plate. During the course of its irradiation, each miniplate experienced many thermal cycles owing to normal startups and shutdowns and power setbacks required by other experiments. Fuel meat centerline temperatures are estimated to have been between 75 and 125°C during irradiation.

The ORR conditions for the full-sized elements were basically the same as for the miniplates. Although the elements were not cycled through the core in a normal pattern, they did experience irradiation in a variety of typical core positions. It is estimated that each element produced ~1.3 MW during its first cycle of irradiation, with a peak-to-average power density and heat flux factor of no more than 1.5. It is estimated that the peak fuel meat temperatures were between 110 and 130°C during the early cycles of irradiation. Average fuel meat temperatures are estimated to have been ~20 to 25°C less. The accessible channel gaps were measured at various times during the irradiation of the elements (following each cycle beyond 50% burnup). Conditions in SILOE were similar to those in the ORR.

5.2 Test Results

The miniplates and elements irradiated in the ORR were subjected to an extensive series of postirradiation examinations following suitable periods of cooling. The key examinations were thickness and volume measurements to assess the swelling of the fuel meat, metallography to assess the condition of the fuel meat, and blister threshold temperature measurements. Gamma scans were performed to provide fission density profiles and plate-to-plate fission density normalization, and uranium and plutonium isotopic analyses of selected samples were performed to provide absolute burnup information. As described

in Appendix G of Ref. 30, calculated ^{235}U fission fractions were used to convert ^{235}U fission densities to the total fission densities reported below.

5.2.1 General

The irradiations of all miniplates and elements proceeded without incident in the ORR. No indications of fission product leaks from the plates were detected. Profiles of channel gaps of the elements remained essentially unchanged during the course of the irradiations, indicating no abnormal swelling or warping of the plates. The miniplates which have been examined thus far, and for which results will be presented below, ranged in ^{235}U burnup from 39 to 96%. Most of the miniplates were irradiated to high burnups in order to establish failure thresholds. Three of the six ORR elements were irradiated to burnups in the normal range for the ORR. The other three, one from each fabricator, were irradiated to ~80% average burnup. Peak burnups in these elements were ~98%. The SILOE element had reached an average burnup of 54%, also without incident, before an extended outage interrupted its irradiation.[32] Except when specifically noted, the data discussed below are from the miniplates and the six elements irradiated in the ORR.

Visual examinations in the hot cells showed the ORR elements to be in excellent condition. No abnormal conditions were observed. Within the accuracy of the in-cell measurements, the dimensions were within the envelope of tolerances allowed for as-fabricated dimensions. In-cell coolant channel gap thickness measurements confirmed the results of the in-pool measurements. Visual examination of the plates following element disassembly revealed no evidence of blisters, excessive swelling, or any other unusual condition.

5.2.2 Fuel Meat Swelling and Microstructure

5.2.2.1 Miniplates

Fuel meat swelling data obtained from immersion density measurements on the uranium silicide miniplates which have been examined to date are summarized in Table IV. These data indicate that the swelling as a function of fission density increases from USi to U_3Si_2 to U_3Si. Data for each of the U_3Si_2 miniplates irradiated are listed in Table V. Four of these miniplates (A87, A89, A90, and A93) have now experienced an estimated 7.5% additional burnup following their initial examinations and are currently being re-examined. Thickness measurements indicate that swelling has remained stable.

A much clearer picture of the swelling behaviors of the various uranium silicides is obtained by calculating the swelling of the fuel particles themselves, assuming that the as-fabricated porosity has been completely filled.

Table IV. Summary of Swelling Data for Uranium Silicide Dispersion Fuels (From PIE of Miniature Fuel Plates)

Fuel Type	Fabricator*	Density Range, Mg/m^3 Low	Density Range, Mg/m^3 High	Enrichment	No. of Plates	Fission Density Range, $10^{27}/m^3$ Low	Fission Density Range, $10^{27}/m^3$ High	Fuel Meat Swelling Range, % $\Delta V/V_m$ Low	Fuel Meat Swelling Range, % $\Delta V/V_m$ High
USi	A	3.86		19.8	1		0.8	0.3	
USi	A	3.81	3.90	40.1	3	2.7	2.8	3.2	6.0
U_3Si_2	A	3.72	3.76	19.9	4	1.6		3.7	4.9
U_3Si_2	A	3.72	3.75	19.9	2†	1.8		6.8	7.1
U_3Si_2	A	5.10	5.20	19.8	5	1.0	2.1	0.0	3.3
U_3Si_2	A	5.60	5.67	19.8	6	2.3		0.1	2.9
U_3Si_2	A	3.94	3.95	40.1	2	1.5	2.5	0.7	11.6
U_3Si_2	A	5.13	5.18	40.1	2	1.8		1.1	2.1
U_3Si_2	A	1.66		93.0	2	1.4	2.3	4.9	11.6
U_3Si	A	4.79	4.83	19.9	5	0.7		0.1	0.8
U_3Si	A	4.77	4.81	19.9	6	2.0	2.2	8.9	11.8
U_3Si	C	5.18	5.20	19.8	2	2.2		10.3	11.4
U_3Si	A	5.65	5.72	19.9	4	1.9		0.7	7.6
U_3Si	A,C	6.10	6.33	19.8	5	2.5	2.6	20.4	38.8**
U_3Si	N	6.89	6.93	19.4	6	2.5		13.3	21.7
U_3Si	A	7.10	7.16	19.8	3	2.6		38.9**	39.1**
U_3Si	A	4.51		40.1	1	2.0		10.3	
U_3Si	A	6.23	6.40	40.1	3	2.4	2.6	9.6	39.6**
U_3Si	A	1.98		92.6	2	1.7		8.8	9.7

*Fabricators: ANL, NUKEM, CNEA.

**Indicates that plates were in various stages of breakaway swelling.

†These two plates, part of the preceding group of plates, were irradiated further following initial postirradiation examination.

Table V. U_3Si_2 Miniplate Swelling Data Summary

Plate No.*	U Dens., Mg/m^3	Fuel Vol. Fraction, %	Fuel Meat Porosity, %	^{235}U Burnup, %	Fuel Meat Fission Dens., $10^{27}/m^3$	Fuel Particle Fission Dens., $10^{27}/m^3$	Fuel Meat Swelling, vol%	Fuel Particle Swelling, vol%
A32	3.8	33.3	4.5	90	1.6	4.8	3.8	25
A34	3.8	33.4	4.3	90	1.6	4.8	4.1	25
A36	3.8	33.3	4.5	90	1.6	4.8	4.3	26
				96	1.8	5.5	7.1	35
A46	3.7	33.1	5.2	90	1.6	4.8	3.7	27
				96	1.8	5.5	6.8	36
A100	5.2	46.2	8.5	42	1.0	2.1	0.0	≤18
A85	5.0	45.4	10.3	79	1.8	4.2	1.6	26
A99	5.2	45.9	9.1	79	1.9	4.2	2.0	24
A87	5.1	45.6	9.8	85	2.1	4.6	3.3	29
A88	5.2	45.8	9.5	85	2.1	4.6	2.6	26
A89	5.6	49.8	13.4	85	2.3	4.6	0.9	29
A90	5.6	49.9	13.3	85	2.3	4.6	0.2	27
A91	5.6	49.7	13.5	85	2.3	4.6	0.1	27
A92	5.6	50.0	12.9	85	2.3	4.6	1.5	29
A93	5.6	50.0	13.0	85	2.3	4.6	0.4	26
A94	5.7	50.4	12.4	85	2.3	4.6	2.9	30
A123M	4.0	35.1	4.2	42	1.5	4.2	0.7	≤14
A124M	3.9	35.0	4.3	69	2.5	7.1	11.6	45
A125M	5.1	45.6	11.8	39	1.8	3.9	2.1	30
A126M	5.2	46.0	11.0	39	1.8	3.9	1.1	26
A121H	1.7	14.7	0.8	41	1.4	9.3	4.9	38
A122H	1.7	14.7	0.8	69	2.3	15.7	11.6	84

*All plates LEU except those with plate number ending in M (MEU) or H (HEU).

The general trends of these data and, for comparison, data for UAl_x,[33] are shown in Fig. 9. The swelling of UAl_x, USi, and U_3Si_2 fuel particles is very stable, being a linear function of the fission density to fission densities well beyond those which can be achieved in LEU fuel (2.4, 5.0, and 5.8 × 10^{27} f/m^3 in the fuel particles of UAl_x, USi, and U_3Si_2, respectively). On the other hand, U_3Si fuel particles in highly loaded fuel plates exhibit an unstable behavior, called breakaway swelling, for fission densities greater than ~4.5 × 10^{27} f/m^3 (~65% ^{235}U burnup for LEU).* The swelling rates per unit fission density of U_3Si_2 and UAl_x fuel particles are the same within the accuracy of the data. The slopes of the linear swelling curves are 4.8%, 6.0%, and 6.2% per 10^{27} f/m^3 for USi, UAl_x, and U_3Si_2, respectively. These data were derived for 40 vol% loadings of USi, 28 to 36 vol% loadings of UAl_x, and 45 to 50 vol% loadings of U_3Si_2. The UAl_x was fully enriched, and the uranium silicides were low enriched. The data of Table V indicate that the slope of the U_3Si_2 swelling curve may be marginally lower for lower fuel volume loadings. Given the fuel particle swelling rate, the fuel volume fraction, and the as-fabricated porosity, the meat swelling for a given fission density can be reliably predicted.

An example of the meat microstructure of a U_3Si_2 miniplate after >90% burnup is shown in Fig. 10. Some of the noteworthy features in this optical micrograph are the absence of fission gas bubbles and the fact that all of the as-fabricated porosity has been consumed by fuel particle swelling. Fuel-aluminum interaction was limited to a narrow zone around the U_3Si_2 particles with a thickness about equal to the range of fission product recoils in aluminum. SEM examination of fractured fuel particles reveals a gas bubble morphology typical of pure U_3Si_2, as shown in Fig. 11. The very uniform distribution of small gas bubbles that show no tendency to interlink is the reason for the stable swelling behavior of U_3Si_2.

---

*The fuel particle swelling curve for another fuel commonly used in aluminum-matrix dispersions today, U_3O_8, is quite similar to the U_3Si curve for highly loaded fuel plates. (Note that the maximum fission density achievable in low-enriched U_3O_8 is 3.6 × 10^{27} f/m^3.) Although the swelling mechanism in U_3O_8 is different than that in U_3Si,[34] the occurrence of breakaway swelling in either requires fission gas bubble growth and interlinkage across extended areas of the fuel meat. If enough aluminum matrix surrounds the fuel particles (i.e., if the fuel volume loading is low enough) to restrain the expansion of fission gas bubbles and/or to prevent bubble linkage from particle to particle, breakaway swelling does not occur. Data for such low-loaded plates lie well to the right of the U_3Si curve shown in Fig. 9.

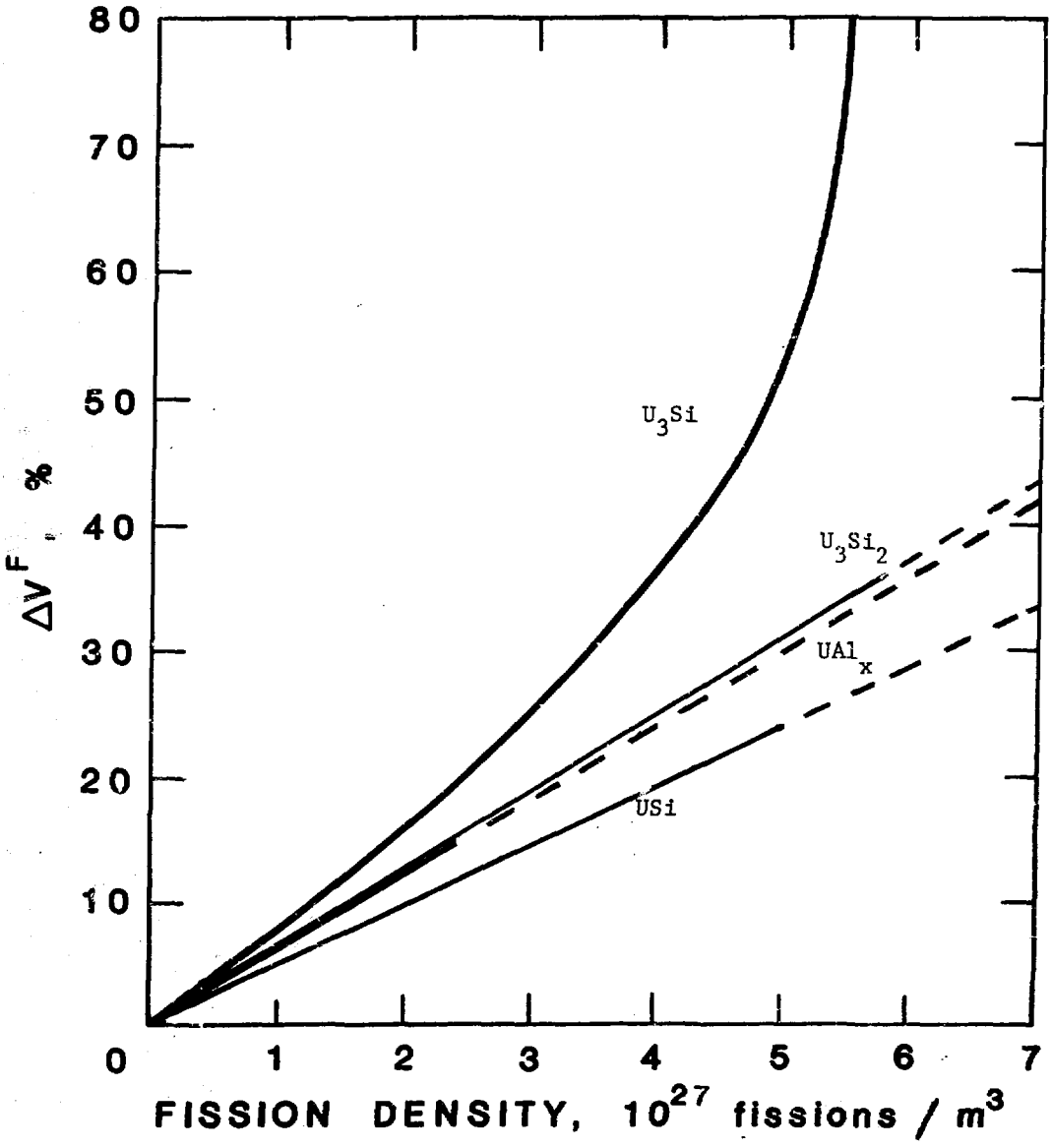

Fig. 9. Swelling of Uranium Silicide and UAl_x Fuel Particles vs. Fission Density in the Particle. Dashed Lines Indicate Fission Densities Not Attainable in LEU Fuel.

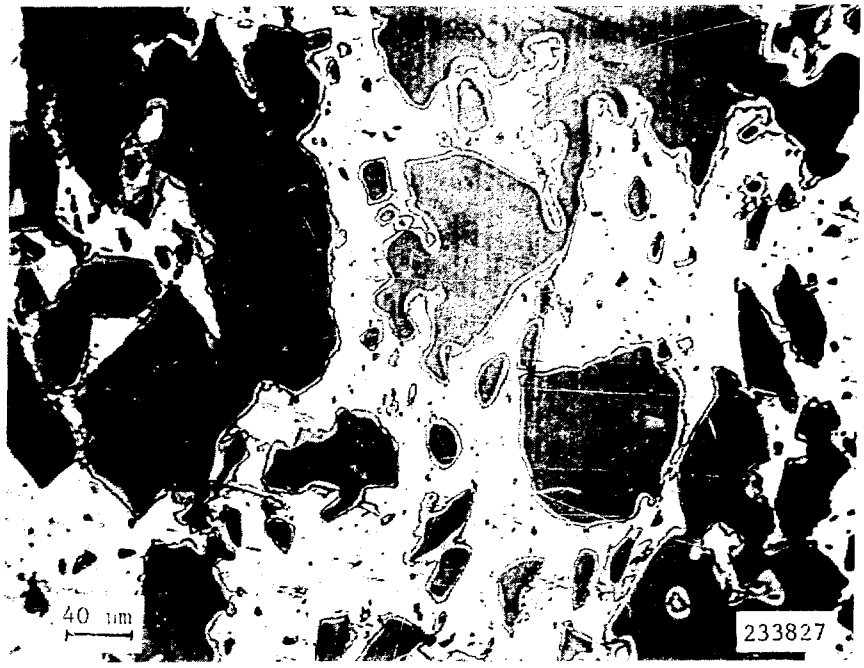

Fig. 10. Meat Microstructure of U_3Si_2 Miniplate After 90% Burnup (Bu).

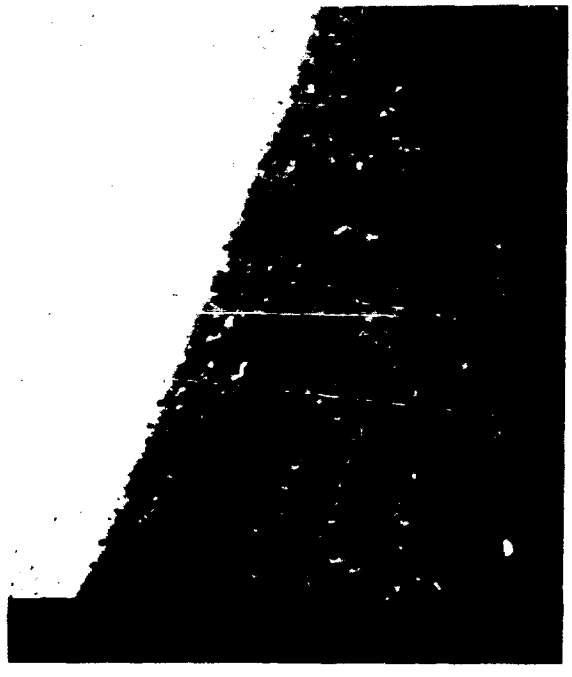

Fig. 11. Fission Gas Bubble Morphology in U_3Si_2 After 90% Bu.

The microstructural changes in U_3Si miniplates resulting from irradiation to high burnups are quite different, as shown in Fig. 12. Fission gas bubbles are clearly visible in the optical micrograph. The bubble morphology, more clearly shown in the SEM images in Fig. 13, reveals a basic difference in fission gas behavior between U_3Si and U_3Si_2. The fission gas bubbles in U_3Si are not uniformly distributed and vary widely in size. The large bubbles are growing rapidly and interlinking, resulting in a much larger fuel swelling rate than that of U_3Si_2. As will be shown in the next section, the fuel in the full-sized U_3Si_2 plates exhibits characteristics of both U_3Si_2 and U_3Si.

5.2.2.2 Full-Sized Plates and Elements

Average thickness changes of plates from the U_3Si_2 elements irradiated in the ORR are shown in Table VI. Although not nearly as accurate a measure of the fuel meat swelling as the volume measurements performed on the miniplates, thickness measurements do show the general trends of the swelling. Note that thickness changes always overestimate the actual volume swelling of the fuel meat because thicknesses between high points of the cladding surfaces are measured. Any warping or twisting of the plate tends to increase the apparent thickness. At 98% burnup ($\sim 2.4 \times 10^{27}$ f/m^3) the thickness increases are small compared to tolerances for the as-fabricated channel gap thicknesses. Similar results were obtained for the individual U_3Si_2 plates irradiated in SILOE. For example, plates with 5.2 Mg U/m^3 had swelled 25 μm at a fission density of 1.4×10^{27} f/m^3 and 45 μm at 2.2×10^{27} f/m^3.

Fuel meat microstructures of plates from the two B&W elements are shown in Figs. 14-16. At 31% burnup a large amount of as-fabricated porosity remains, and no fission gas bubbles are visible in the fuel particles. At 71% burnup most of the porosity has been filled, and fission gas bubbles are visible in scattered fuel particles. These fission gas bubbles have grown considerably by 97% burnup, where the measured thickness increase was 46 μm. The SEM images in Figs. 17-20 show examples of the fission gas behavior in three distinct fuel phases. The major phase has a bubble morphology characteristic of pure U_3Si_2 (Fig. 20), while parts of several fuel particles have either a characteristic U_3Si bubble morphology (Figs. 17 and 18) or, as shown in Fig. 19, a total absence of bubbles and apparent brittle properties reminiscent of UAl_4.

The different fission gas behavior in parts of the ostensibly pure U_3Si_2 fuel grains was understood through the results of a detailed microscopic examination of an unirradiated fuel plate. The fuel particles were found to contain both U_3Si and U_{ss}. The B&W fuel had not been heat treated, so U_{ss} resulting from inhomogeneities in the as-cast ingot was not converted to U_3Si. The small amount of U_3Si in the unirradiated fuel meat was undoubtedly formed

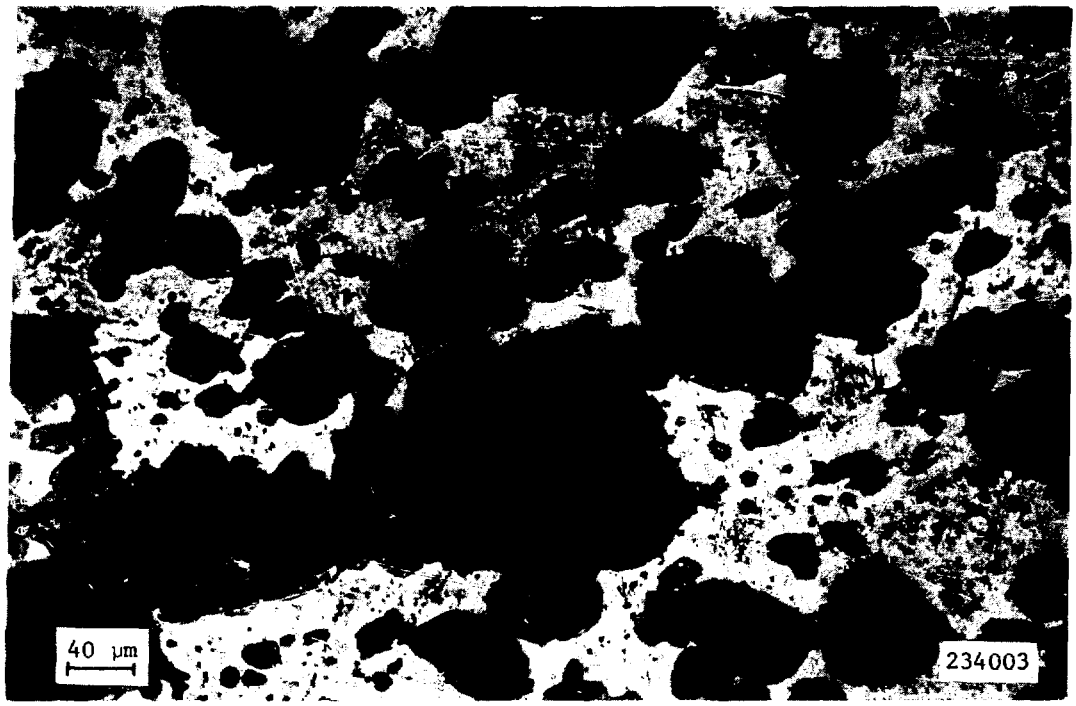

Fig. 12. Meat Microstructure of U_3Si Miniplate After 90% Bu.

Fig. 13. Fission Gas Bubble Morphology in U_3Si After 90% Bu.

Table VI. Average Thickness Increase and Burnup of ORR U_3Si_2 Test Elements

Element No.	Low-Burnup End			Peak-Burnup Region			Element-Average Burnup, %
	Burnup, %	Thickness Increase, mils	µm	Burnup, %	Thickness Increase, mils	µm	
BSI-201	28	0	0	69	1.5	38	54
BSI-202	53	0	0	97	1.8	46	77
CSI-201	32	0.1	3	66	1.7	43	52
CSI-202	55	0.9	23	98	4.4	112	82
NSI-201	19	0.7	18	46	1.0	25	35
NSI-202	53	1.2	30	97	4.1	104	82

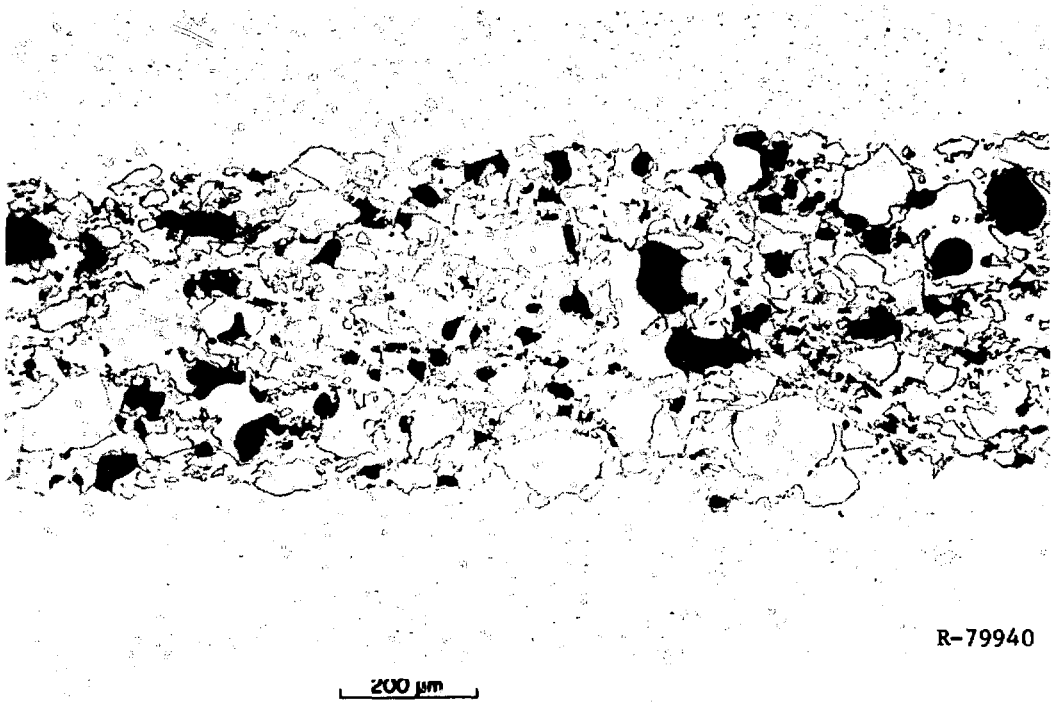

Fig. 14. Meat Microstructure of Plate BSI-201, at 31% Bu.

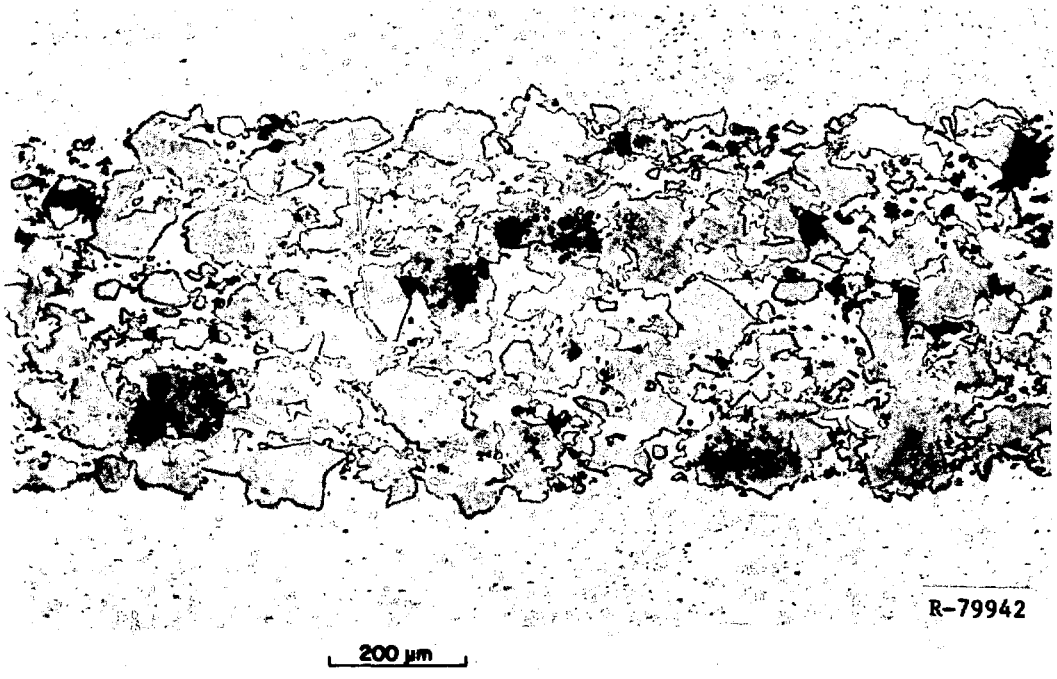

Fig. 15. Meat Microstructure of Plate BSI-201, at 71% Bu.

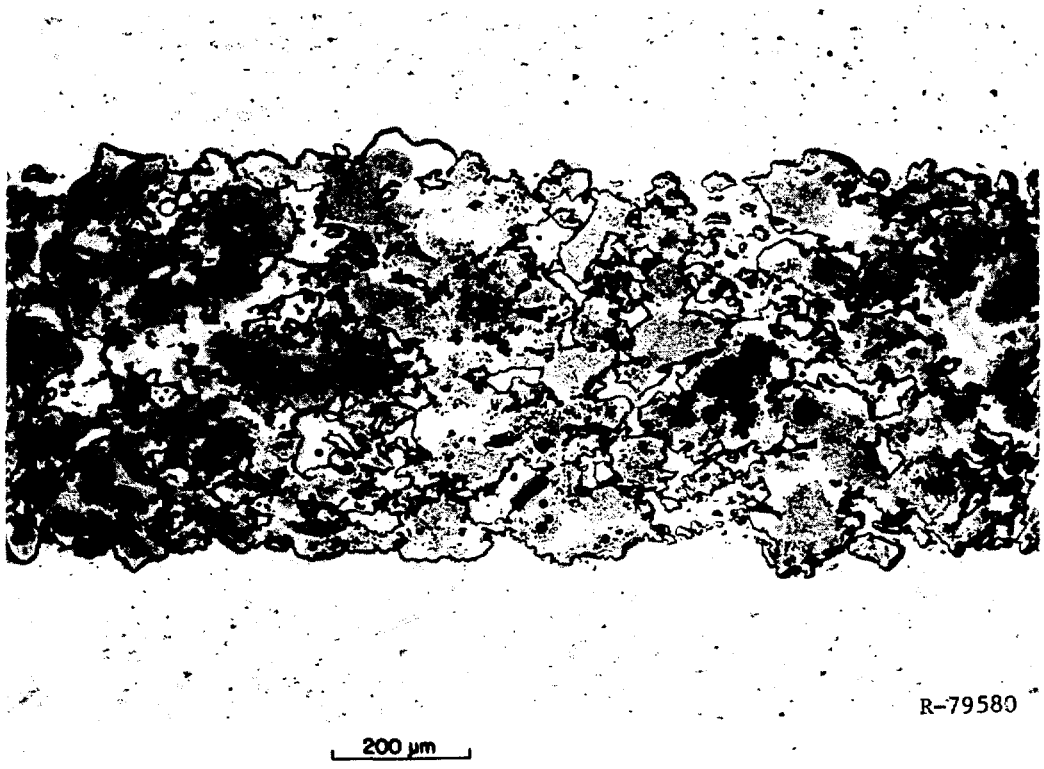

Fig. 16. Meat Microstructure of Plate BSI-202, at 97% Bu.

Fig. 17. SEM Image of Fuel Meat of Plate BSI-202, at 97% Bu, Showing Various Bubble Morphologies.

Fig. 18. Idem Fig. 17.

Fig. 19. Idem Fig. 17.

Fig. 20. Idem Fig. 17.

during hot rolling and blister testing. Therefore, the U_3Si and U_3Si_2 show their characteristic irradiation behaviors, and the U_{ss} presumably reacts with Al during irradiation to form the stable UAl_4 compound, in which fission gas bubbles have never been observed. Therefore, the presence of U_{ss} in the as-fabricated fuel does not appear to be detrimental to the performance of the fuel plate. Even though the U_3Si was found to contain all the larger bubbles, its amount was such that no continuous network of large bubbles could develop, even at the very high burnup attained in these plates. It has been established in miniplate irradiations that interparticle linkup of larger bubbles is a prerequisite for possible large swelling in U_3Si.

Fuel meat microstructures of plates from the two CERCA elements are shown in Figs. 21-23, at burnups similar to those of the B&W plates. The much lower residual porosity seen in Fig. 21 reflects the 4% porosity in the unirradiated CERCA plates compared to 9 to 10% in the B&W plates. The high-burnup (97%) end of plate CSI-202 had a measured thickness increase of 112 μm, more than twice that of the B&W plate. The fuel microstructure shows basically the same two-phase fission gas morphology seen in plate BSI-202 with the U_3Si-type bubbles more evenly distributed throughout the fuel. The total fission gas bubble volume appears to be significantly larger than that seen in the B&W plates, as would be expected from the much larger thickness increase experienced by the CERCA plates. Some of this larger thickness increase is attributable to the smaller porosity of the CERCA fuel meat relative to the B&W fuel meat, but the largest part of the difference undoubtedly owes to a larger amount of U_3Si in the CERCA plates.

The fission gas bubble behavior is, in fact, consistent with the as-fabricated fuel microstructure. The CERCA fuel did contain more U_3Si than did the B&W fuel; however, it was more finely distributed than in the B&W fuel. The CERCA fuel did not contain U_{ss} because it had been heat treated, hence the absence of the UAl_4-like phase in the irradiated plate.

Fuel meat microstructures at three different burnups in plates from the NUKEM elements are shown in Figs. 24-26. The appearance is very similar to that of the CERCA fuel meat. The fuel consisted of U_3Si_2 with a somewhat coarsely distributed (compared to the CERCA fuel) second phase. The amount of this second phase, identified as U_3Si, appeared to be the highest of the three, albeit still minor. The high-burnup (96%) end of plate NSI-202, shown in Fig. 26, had a measured thickness change of 104 μm. The fission gas bubble morphology is rather similar to that of the other high-burnup plates, exhibiting a two-phase behavior. The SEM images of a U_3Si_2 fuel particle with low (24%) burnup, shown in Figs. 27 and 28, show that at this burnup the U_3Si_2 particles appear very similar to UAl_4 particles.

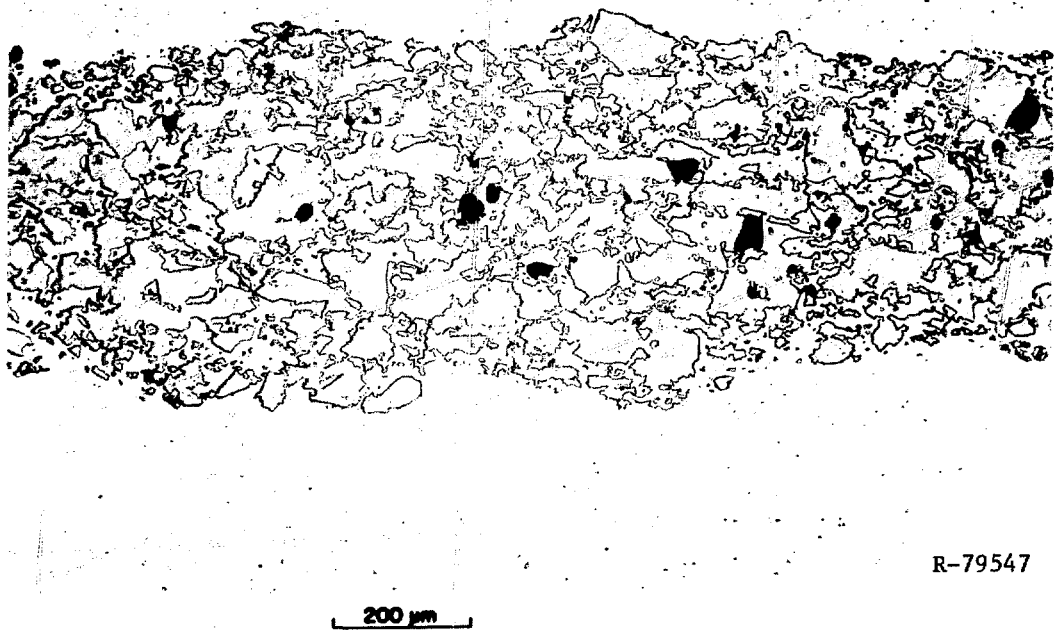

Fig. 21. Meat Microstructure of Plate CSI-201, at 33% Bu.

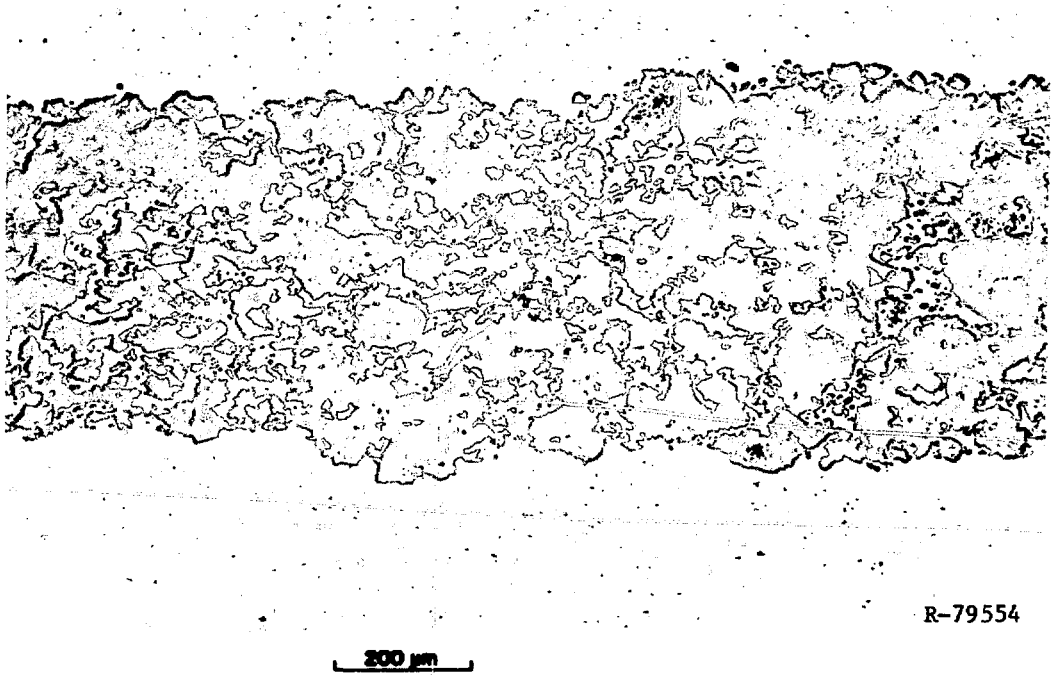

Fig. 22. Meat Microstructure of Plate CSI-201, at 67% Bu.

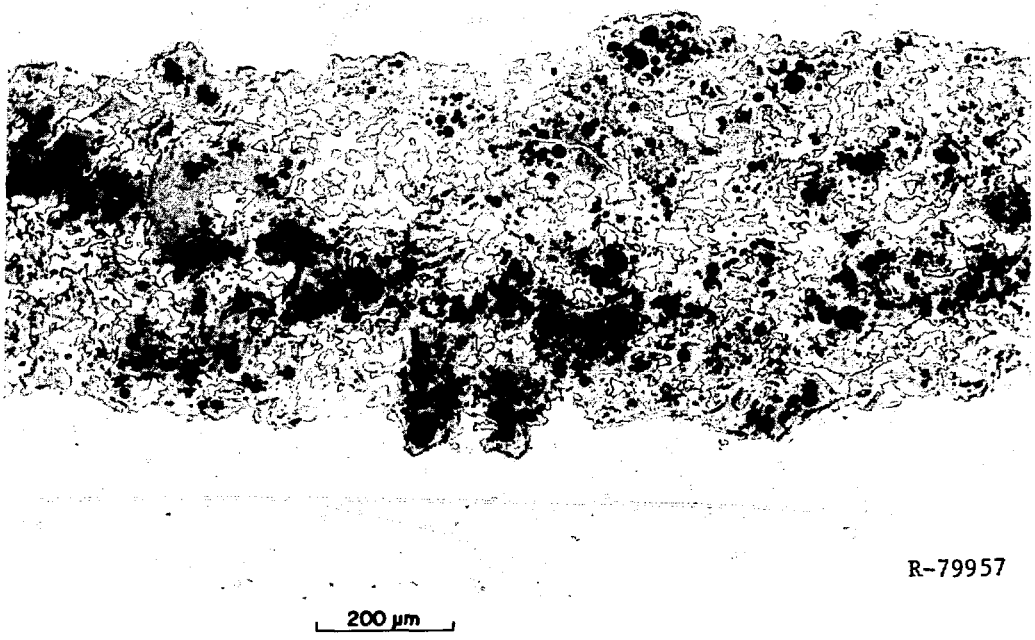

Fig. 23. Meat Microstructure of Plate CSI-202, at 97% Bu.

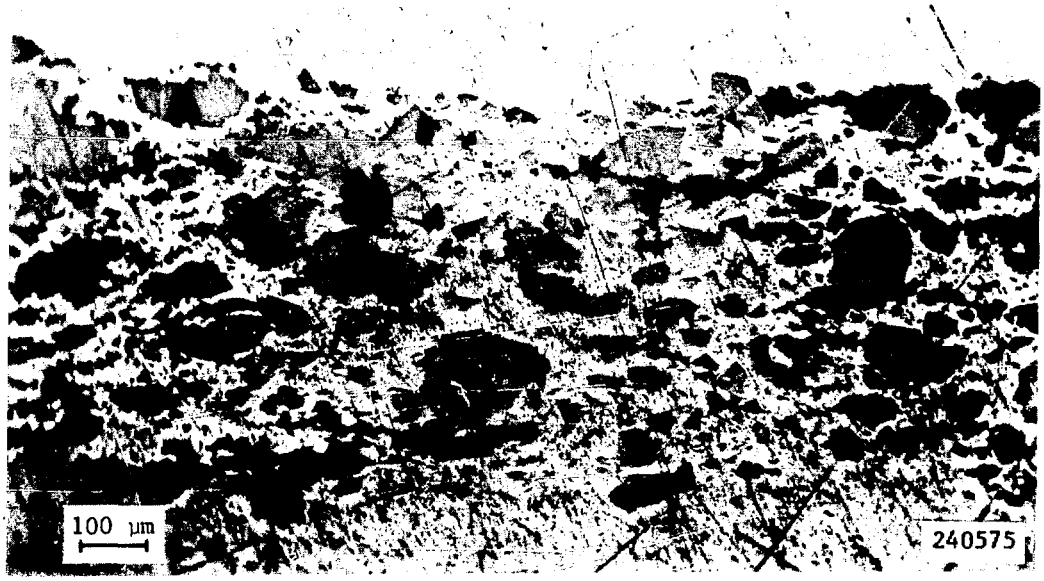

Fig. 24. Meat Microstructure of Plate NSI-201, at 24% Bu.

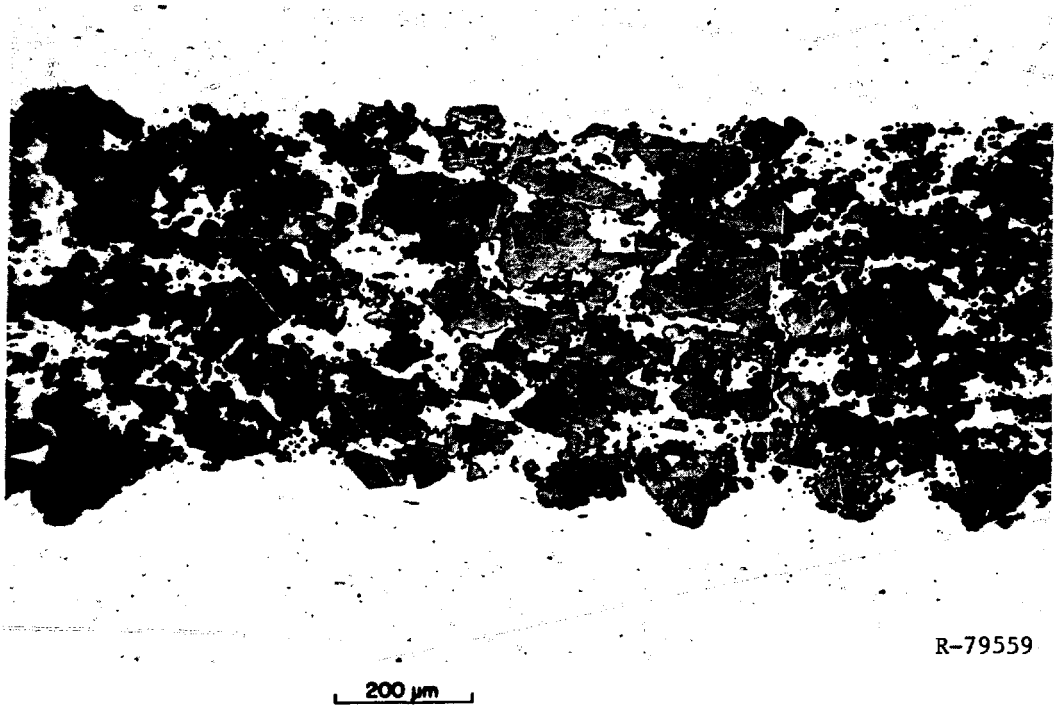

Fig. 25. Meat Microstructure of Plate NSI-202, at 54% Bu.

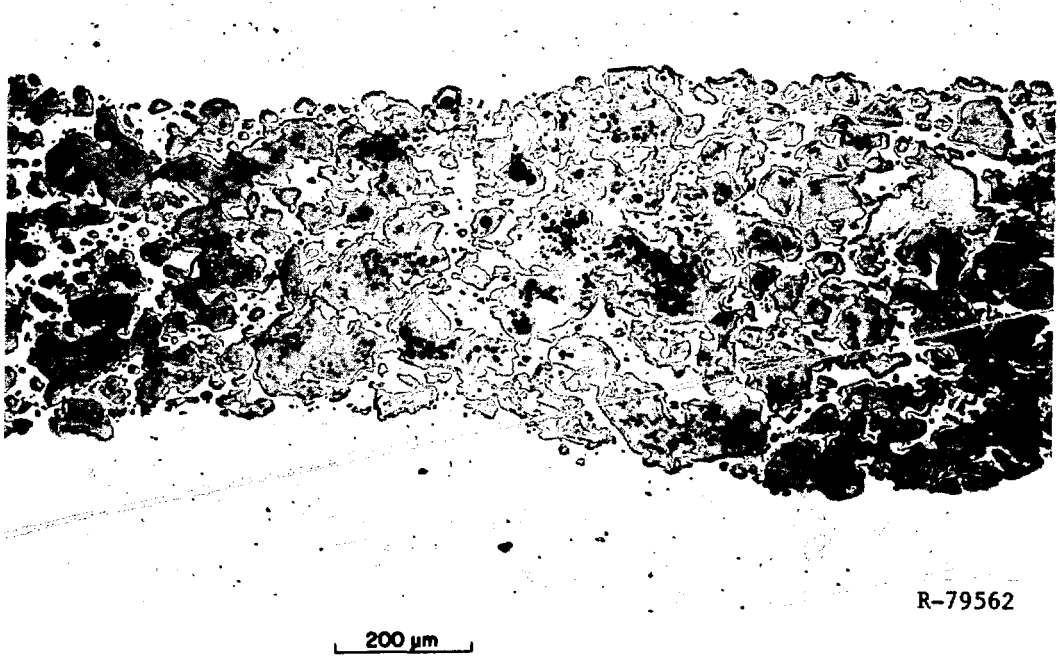

Fig. 26. Meat Microstructure of Plate NSI-202, at 96% Bu.

In conclusion, the metallographic observations are consistent with the relatively small plate thickness increases experienced during irradiation. The swelling is primarily caused by formation of two distinct fission gas bubble morphologies. The by-far-major phase, U_3Si_2, developed a very uniform and dense distribution of submicron-sized bubbles, characteristic of this fuel. The second silicide phase, U_3Si, which occurred in different amounts in the three fuels, developed its characteristic coarse, nonuniform bubble morphology. The amount of U_3Si and its larger swelling account, with the as-fabricated porosity, for the variability in overall plate swelling between plates of the different fabricators. The similarity of the average thickness changes in the high-burnup regions of elements CSI-202 and NSI-202 suggest that differences in bubble morphology may not be as great as comparison of Figs. 23 and 26 seems to indicate. Since only one section from the high-burnup region of CSI-202 was examined, there is a possibility that the section was atypical.

The non-U_3Si_2 phases present in the fuels are a result of fabrication practices. It is not possible, on a commercial scale, to produce a perfectly homogeneous alloy with the exact composition of a line compound such as U_3Si_2. Heat treatment of the ingots employed by CERCA and NUKEM but not by B&W would explain the absence of U_{ss} in the CERCA and NUKEM fuel. However, the U_{ss} phase found in B&W plates evidently reacted with aluminum during irradiation and had no deleterious effect on the swelling behavior of the fuel.

The minor differences in postirradiation microstructure of the fuel meat of the six ORR test elements reflect differences in fabrication practices of the manufacturers at the various times of fabrication. For example, when NUKEM fabricated the first two U_3Si_2 elements, it was not known that U_3Si behaved differently under irradiation than U_3Si_2 and that it might be desirable to control the amount of U_3Si in the fuel powder. Procedures developed during the course of U_3Si_2 development should result in a more uniform product now and in the future.

The discussion of this section has concentrated on differences in irradiation behavior in order to foster an understanding of the processes at work. However, the completely satisfactory behavior of the six U_3Si_2 test elements in the ORR, three of which were operated to ~80% burnup, must be emphasized.

5.2.3 Blister Threshold Temperature

The postirradiation blister threshold temperature has been used traditionally as an indicator of the relative failure resistance of plate-type dispersion fuels. The U_3Si_2 (and U_3Si) miniplates blistered at temperatures in the range of 515 to 530°C, except for very highly loaded U_3Si miniplates

which, at the threshold of breakaway swelling, blistered at 450 to 475°C. Thirteen plates from the full-sized elements were blister tested. Blister temperatures were in the range of 550 to 575°C. The blister threshold temperature appears to be insensitive both to burnup and to fuel volume loading. These temperatures are at least as high as those measured for highly enriched UAl_x and U_3O_8 dispersion fuels in use today.[33,35]

5.2.4 Fission Product Release

Over the years several studies of fission product release from plate-type reactor fuels have been done, first for plates with U-Al alloy meat and later for plates with UAl_x and U_3O_8 dispersion meats. Results of these experiments have been summarized in Refs. 36 and 37. As part of the development of high-density fuels under the RERTR Program, some fission product release measurements of limited scope have been performed.

Measurements using UAl_x miniplates were performed at ORNL in collaboration with the Kyoto University Research Reactor Institute primarily to determine the threshold temperature for fission product release and to measure release rates above that temperature.[38] These tests showed that the first significant release of gaseous fission products occurred when the fuel plate blistered. Another significant release occurred at about the solidus temperature of the cladding, and a third significant release occurred at about the UAl_4-Al eutectic temperature. Only very small releases of ^{131}I and ^{137}Cs were detected; however, since the system was designed primarily for the measurement of gaseous fission products, it is likely that only a small fraction of the total quantity released was detected.

Similar measurements, using the same equipment, were made using U_3O_8 and U_3Si miniplates, with similar results.[39] The first release of gaseous fission products was detected when the plates blistered, at 500°C for the U_3Si plate and at 550°C for the U_3O_8 plates. Essentially all of the gaseous fission products had been released by the end of the test at 650°C. From the amounts of Cs detected in the traps and from visual observations of deposits on the sample holder following the 650°C test, it was determined that much more Cs was released from the U_3Si plate than from the U_3O_8 plate.

It is expected that the fission product release characteristics of U_3Si_2 dispersed in aluminum are similar to those of U_3Si. The major release of fission gas occurred at about the aluminum melting temperature, where it is known from the DTA studies discussed in Section 4.5 that both U_3Si_2 and U_3Si fully react with the aluminum. The disruption of the fuel structure during the reaction undoubtedly enhances the release of the volatile and solid fission products. Release fractions in U_3Si_2 fuel might be less than those in U_3Si

fuel because the exothermic energy release in the U_3Si_2-Al reaction is less than that in the U_3Si-Al reaction. It is also possible that release rates of fission gas below the threshold of the exothermic reaction might be less for U_3Si_2 than for U_3Si, since the bubble morphologies of the irradiated fuel particles indicate that fission gas mobilities in U_3Si_2 are considerably less than in U_3Si.

Although no quantitative release data were obtained for I and Cs, the data for U-Al alloy and U_3O_8 dispersions[37,40] provide guidance in arriving at release fractions for safety analyses. These data indicate that up to 25% of the Cs and 70% of the I are released at 700°C in air. The presence of steam lowers the release fraction somewhat. There is certainly no reason to think that release fractions would be smaller in the uranium silicides, and for Cs, there is evidence that the release fraction could be considerably larger. Therefore, reasonable bounds for the release fractions of Cs and I are 25 to 100%. The uncertainty in this quantity is quite small compared to the uncertainty in the attenuation factor for transport of these fission products from the molten fuel to the containment or confinement boundary.

5.3 Demonstration of Commercially Fabricated U_3Si_2 Fuel Elements in the ORR

Following successful irradiation testing of the six fuel elements in the ORR described above, a whole-core demonstration of U_3Si_2 fuel was conducted in the ORR to provide both reactor physics data and proof that commercially fabricated elements would perform well. The fuel elements for the demonstration were essentially identical to the test elements and were fabricated by B&W, CERCA, and NUKEM. In addition the shim rods contained fuel followers with 15 fuel plates loaded to 3.5 Mg U/m^3. The fuel elements and shim rods were moved about the core in the normal ORR pattern.

At the end of the demonstration in March 1987, 68 fuel elements and eight fuel followers had been irradiated, with average burnups (estimated from calculations) as shown in Table VII. All elements and followers appear to have performed flawlessly. Channel gap measurements, made periodically on a few elements from each fabricator, indicated no significant changes.

5.4 Reprocessing of Uranium Silicide Fuels

Currently, most spent plate-type research reactor fuel elements from the free world are reprocessed in the U.S. to recover unburned ^{235}U. In order to demonstrate the reprocessability of uranium silicide fuels, studies were conducted at the Savannah River Laboratory for the RERTR Program.[41] Both unirradiated and irradiated fuel samples were tested. The studies demonstrated that uranium silicide fuels can be successfully reprocessed at the

Table VII. ^{235}U Burnup of ORR U_3Si_2 Demonstration Fuel Elements*

Range, %	Number of 19-Plate Standard Fuel Elements			
	CERCA	NUKEM	Babcock & Wilcox	Total
>50	2	2	2	6
45-50	6	3	2	11
40-45	2	6	4	12
35-40	1	1	4	6
30-35	0	1	3	4
25-30	1	2	0	3
20-25	5	1	0	6
15-20	1	2	2	5
10-15	0	1	7	8
5-10	2	1	4	7
Total:	20	20	28	68

Range, %	Number of 15-Plate B&W Fuel Followers
70-75	2
55-60	2
35-40	2
10-15	2
Total:	8

*Based on REBUS-3 calculations performed by M. M. Bretscher and R. J. Cornella.

Savannah River Plant. Subsequently the U.S. Department of Energy agreed to accept spent LEU silicide fuels for disposition on essentially the same terms as for the current HEU fuels.[42]

6. FABRICATION SPECIFICATIONS

A number of the findings from the tests of U_3Si_2 dispersion fuels discussed above have direct bearing on requirements of fabrication specifications. Some of these, related directly to the fuel powder or to general properties of high-density fuels, are discussed briefly below, with recommendations.

6.1 U_3Si_2 Powder

6.1.1 Composition

As indicated in Table I, the silicon content of the U_3Si_2 in the miniplates and test elements ranged from 7.2 to 7.7 wt%. For the U_3Si_2 elements procured for the ORR demonstration, the silicon content ranged from 7.4 to 7.9 wt%. Based upon the results from the test elements, it appears that there is no detrimental effect of up to a few vol% of U_{ss}.

It is recommended that U_3Si_2 fuel be specified at its stoichiometric composition, with a suitable tolerance range: 7.3 ± 0.2 wt%. At 7.1 wt% Si there would be only 1.9 vol% (2.9 wt%) of U_{ss} in homogeneous fuel at equilibrium. At the upper end of the range, there would be 6.5 vol% (5.9 wt%) of USi in the fuel. The use of a slightly higher silicon content, e.g. 7.5 wt%, would considerably reduce the potential amount of U_{ss} in the fuel. However, there appears to be no practical improvement in fuel performance, and the volume loading of fuel required for a given ^{235}U loading would be slightly increased.

It is also recommended that the fuel not be heat treated. Having small amounts of U_{ss} present, which converts primarily to UAl_4, is preferable to having U_3Si present.

It does not appear necessary to have a requirement limiting the amounts of constituent phases per se. Commercial production practices are capable of achieving adequate homogeneity. Therefore, only a test of the average U, Si, and impurity contents is needed to assure a fuel with an acceptably low content of minor phases once the melting process has been qualified.

6.1.2 Impurities

Principal impurities in the fuel for the miniplates and test elements were Al (400 ppm), C (400 ppm), Fe (550 ppm), N (1672 ppm), and O (1290 ppm). No detrimental effects of these impurities were found. In fact, allowing a reasonable amount of surface oxidation to passivate the fuel particles appears prudent. Based upon experience obtained from the ORR demonstration, it recommended that the following impurity levels be accepted: Al (600 ppm), C (1000 ppm), Fe + Ni (1000 ppm), N (1700 ppm), and O (7000 ppm).

6.1.3 Particle Size Distribution

The fines content of the fuels tested ranged between 15 and 40 wt%. There appears to be no detrimental effect of the higher fines content. It is recommended that up to 50 wt% fines be allowed.

The upper limit of particle size in current specifications ranges between 125 and 150 μm. There is no reason based on fuel performance to change this limit. However, a fabricator may find it advantageous to further limit the maximum particle size in order to more easily meet minimum cladding and homogeneity requirements. A 90-μm upper limit is acceptable, based on experience with the CERCA test elements.

6.2 Stray Fuel Particles

It is anticipated that as the use of high-density fuels becomes prevalent, all fabricators will adopt methods to eliminate the possiblity of stray fuel particles. In the meantime, however, it is important not to be overly restrictive in the number of stray fuel particles allowed by the specifications. A fuel-free zone of 0.4- to 0.5-mm width is recommended for the edges and ends of the plates to preclude fission product leaks from the particles. Filing to eliminate particles close to the edges or ends appears to be a viable means of saving a plate which would otherwise be rejected. Fuel particles should not be allowed in the plate identification number area since the cladding thickness is reduced by the numbering process. Smears of very fine fuel particles covering significant areas should be avoided since it is possible that cover-frame bonding might be poor in such areas.

6.3 Fuel Meat Porosity

As discussed previously, the as-fabricated porosity of the fuel meat varies from fabricator to fabricator, probably because of differences in materials and fabrication parameters. For U_3Si_2 at the upper range of fabricability, the porosity varied from 4 to 10 vol% for the ORR test elements. However, the 6% difference in thickness change (~30 μm) attributable to this

difference in porosity is not significant for U_3Si_2 fuel. It is recommended that there be no specific requirement for as-fabricated porosity. If the amount of porosity should be required to be reported as information, only a small sample is needed because the amount of porosity will remain quite constant for a given set of materials and process parameters.

7. SUMMARY AND CONCLUSIONS

As discussed in the preceding sections, extensive tests of the properties of U_3Si_2 dispersion fuel and its irradiation behavior have been performed under the auspices of the RERTR Program. In summary, it has been found that:

1. U_3Si_2 is compatible with the aluminum matrix and cladding. Very little reaction between U_3Si_2 and Al occurs at or below fabrication temperatures. During irradiation this reaction occurs only in the fission fragment recoil zone. The fuel is also compatible with water. No dissolution of the fuel occurred in water boiling at 100°C. U_3Si_2 dispersion fuel can be successfully fabricated with the cladding materials currently used for HEU dispersion fuels, so no question regarding cladding-coolant compatibility is raised.

2. The thermal conductivity of U_3Si_2 dispersion fuel has been measured and found to be similar to those of UAl_x and U_3O_8 dispersion fuels at similar volume loadings of fuel.

3. An exothermic reaction between U_3Si_2 and Al occurs at about the Al melting temperature. The magnitude of the energy release is low enough to be compensated by the Al melting endotherm. The reaction occurs slowly enough (over a period of minutes) to mitigate its consequences in an accident.

4. U_3Si_2 swells very stably under irradiation, at almost the same rate as a function of fission density as UAl_x. Fission gas is contained within the particles in submicron-sized bubbles. Fuel particle swelling is a linear function of the fission density to well beyond the maximum fission density possible in LEU fuel. Test samples containing ~45 vol% fuel showed no evidence of incipient failure at 98% burnup (~2.5×10^{27} f/m^3 in the fuel meat). The presence of minor amounts of other phases which might be present in nominal U_3Si_2 (U_3Si, U_{ss}, and USi) are acceptable. Full burnup of LEU fuel appears feasible.

5. Blister threshold temperatures (515 to >550°C) are at least as high as those of the HEU fuels now being used.

6. Fuel elements irradiated to well beyond normal burnup were dimension-ly stable, indicating that the mechanical properties of Al-clad U_3Si_2 dis-rsion fuel are acceptable.

7. Release fractions of volatile fission products were not measured for anium silicide fuels, but major releases would occur during the exothermic action. Release fractions could not be significantly above the 25 to 70% lues measured for U-Al alloy or U_3O_8 dispersion fuels, being limited, of urse, to 100%.

It is concluded, therefore, that U_3Si_2 dispersion fuel with uranium nsities up to at least 4.8 Mg/m^3 is a suitable LEU fuel for typical plate-pe research and test reactors.

ACKNOWLEDGMENTS

The talents and dedicated efforts of many persons have resulted in the ccessful development and testing of U_3Si_2 dispersion fuel. The contribu-ons of personnel associated with the Materials Processing Group and the pha-Gamma Hot Cells at ANL and with the ORR and the HRLEL at ORNL are atefully acknowledged. We especially thank F. J. Karasek and D. R. Schmitt r their unique contributions to fuel fabrication and E. D. Clemmer for rforming hundreds of channel gap scans throughout the irradiation program. ıally, the guidance of H. R. Thresh, L. A. Neimark, and D. Stahl (during -ly stages of development and testing) has been very much appreciated.

REFERENCES

A. Travelli, "The RERTR Program: A Progress Report," Proc. 1986 Int. Mtg. on Reduced Enrichment for Research and Test Reactors, Gatlinburg, Tennessee, November 3-6, 1986, Argonne National Laboratory Report ANL/RERTR/TM-9 (in press).

G. B. West, M. T. Simnad, and G. L. Copeland, "Final Results from TRIGA LEU Fuel Post-Irradiation Examination and Evaluation Following Long Term Irradiation Testing in the ORR," Proc. 1986 Int. Mtg. on Reduced Enrichment for Research and Test Reactors, Gatlinburg, Tennessee, November 3-6, 1986, Argonne National Laboratory Report ANL/RERTR/TM-9 (in press).

D. F. Sears, L. C. Berthiaume, and L. N. Herbert, "Fabrication and Irradiation Testing of Reduced Enrichment Fuels in Canadian Research Reactors," Proc. 1986 Int. Mtg. on Reduced Enrichment for Research and Test Reactors, Gatlinburg, Tennessee, November 3-6, 1986, Argonne National Laboratory Report ANL/RERTR/TM-9 (in press).

4. F. Cherruau, "The Caramel Fuel in OSIRIS: The Complete Conversion of a High Flux Research Reactor to a Low Enriched Fuel," Proc. Int. Mtg. on Development, Fabrication and Application of Reduced Enrichment Fuels for Research and Test Reactors, Argonne, Illinois, November 12-14, 1980, Argonne National Laboratory Report ANL/RERTR/TM-3 (CONF-801144), pp. 310-318 (August 1983).

5. M. Barnier and J. P. Beylot, "OSIRIS, A MTR Adapted and Well Fitted to LEU Utilization Qualification and Development," Proc. Int. Mtg. on Reduced Enrichment for Research and Test Reactors, Tokai, Japan, October 24-27, 1983, Japan Atomic Energy Research Institute Report JAERI-M 84-073, pp. 256-267 (May 1984).

6. R. F. Domagala, "Phases in U-Si Alloys," Proc. 1986 Int. Mtg. on Reduced Enrichment for Research and Test Reactors, Gatlinburg, Tennessee, November 3-6, 1986, Argonne National Laboratory Report ANL/RERTR/TM-9, in press.

7. R. F. Domagala, T. C. Wiencek, and H. R. Thresh, "Some Properties of U-Si Alloys in the Composition Range U_3Si to U_3Si_2," Proc. 1984 Int. Mtg. on Reduced Enrichment for Research and Test Reactors, Argonne, Illinois, October 15-18, 1984, Argonne National Laboratory Report ANL/RERTR/TM-6 (CONF-8410173), pp. 47-60 (July 1985).

8. A. G. Samoilov, A. I. Kashtanov, and V. S. Volkov, *Dispersion-Fuel Nuclear Reactor Elements*, (1965), translated from the Russian by A. Aladjem, Israel Program for Scientific Translations Ltd., Jerusalem, pp. 54-57 (1968).

9. A. E. Dwight, "A Study of the Uranium-Aluminum-Silicon System," Argonne National Laboratory Report ANL-82-14, p. 29 (September 1982).

10. H. Shimizu, "The Properties and Irradiation Behavior of U_3Si_2," Atomics International Report NAA-SR-10621, p. 14 (July 25, 1965).

11. R. F. Domagala, T. C. Wiencek, and H. R. Thresh, "U-Si and U-Si-Al Dispersion Fuel Alloy Development for Research and Test Reactors," Nucl. Tech. 62, 353-360 (September 1983).

12. T. Görgenyi and U. Huth, "Determination of Cladding Thickness in Fuel Plates for Material Test and Research Reactors (MTR)," presented at Seminar on Research Reactor Operation and Use, Jülich, Fed. Rep. of Germany, September 14-18, 1981.

13. H. W. Hassel and E. Wehner, NUKEM, personal communication (April 1986).

14. G. Thamm, "The German AF-Program Status and Final Activities," Proc. 1986 Int. Mtg. on Reduced Enrichment for Research and Test Reactors, Gatlinburg, TN, November 3-6, 1986, Argonne National Laboratory Report ANL/RERTR/TM-9, in press.

15. K. Bogacik, "Status of LEU Programs at Babcock & Wilcox," *Reduced Enrichment for Research and Test Reactors--Proceedings of an International Meeting, Petten, The Netherlands, October 14-16, 1985*, P. von der Hardt and A. Travelli, Eds., D. Reidel Publishing Company, Dordrecht, pp. 165-173 (1986).

16. S. Nazaré, "Low Enrichment Dispersion Fuels for Research and Test Reactors," J. of Nucl. Materials 124, 14-24 (1984).

17. P. Toft and A. Jensen, "Differential Thermal Analysis and Metallographic Examinations of U_3Si_2 Powder and U_3Si_2/Al (38 w/o) Miniplates," *Reduced Enrichment for Research and Test Reactors--Proceedings of an International Meeting, Petten, The Netherlands, October 14-16, 1985*, P. von der Hardt and A. Travelli, Eds., D. Reidel Publishing Company, Dordrecht, pp. 373-381 (1986).

18. T. C. Wiencek, "A Study of the Effect of Fabrication Variables on the Quality of Fuel Plates," Proc. 1986 Int. Mtg. on Reduced Enrichment for Research and Test Reactors, Gatlinburg, Tennessee, November 3-6, 1986, Argonne National Laboratory Report ANL/RERTR/TM-9, in press.

19. *CRC Handbook of Chemistry and Physics*, 64th Edition, R. C. Weast, Ed., CRC Press, Boca Raton, pp. D-43 and D-44 (1983).

20. R. K. Williams, R. S. Graves, R. F. Domagala, and T. C. Wiencek, "Thermal Conductivities of U_3Si and U_3Si_2-Al Dispersion Fuels," Proc. 19th Int. Conf. on Thermal Conductivity, Cookeville, Tennessee, October 21-23, 1985, in press.

21. R. R. Hobbins, EG&G Idaho, unpublished information (1973).

22. G. L. Copeland and M. M. Martin, "Development of High-Uranium-Loaded U_3O_8-Al Fuel Plates," Nucl. Tech. 56, 547 (1982).

23. T. C. Wiencek, R. F. Domagala, and H. R. Thresh, "Thermal Compatibility Studies of Unirradiated Uranium Silicide Dispersed in Aluminum," Nucl. Tech. 71, 608-616 (1985).

24. C. E. Weber, "Progress on Dispersion Elements," *Progress in Nuclear Energy*, Ser. V, 2, Pergamon Press, N.Y. (1959).

25. R. F. Domagala, T. C. Wiencek, J. L. Snelgrove, M. I. Homa, and R. R. Heinrich, "Differential Thermal Analysis of U_3Si-Al and U_3Si_2-Al Reactions," Argonne National Laboratory Report ANL/RERTR/TM-7 (October 1984) and Am. Cer. Soc. Bull. 65(8), 1164-70 (1986).

26. S. Nazaré, "Reaction Behavior of U_xSi_y- and U_6Fe-Al Dispersions," Proc. 1984 Int. Mtg. on Reduced Enrichment for Research and Test Reactors, Argonne, Illinois, October 15-18, 1984, Argonne National Laboratory Report ANL/RERTR/TM-6 (Conf-8410173), pp. 39-46 (July 1985).

27. A. E. Pasto, G. L. Copeland, and M. M. Martin, "Quantitative Differential Thermal Analysis Study of the U_3O_8-Al Thermite Reaction," Am. Cer. Soc. Bull., 61(4), 491-496 (1982).

28. J. D. Fleming and J. W. Johnson, "Aluminum-U_3O_8 Exothermic Reactions," Nucleonics, 21(5), 84-87 (May 1963).

29. R. L. Senn and M. M. Martin, "Irradiation Testing of Miniature Fuel Plates for the RERTR Program," Oak Ridge National Laboratory Report ORNL/TM-7761 (July 1981).

30. G. L. Copeland, R. W. Hobbs, G. L. Hofman, and J. L. Snelgrove, "Performance of Low-Enriched U_3Si_2-Aluminum Dispersion Fuel Elements in the Oak Ridge Research Reactor," Argonne National Laboratory Report ANL/RERTR/TM-10 (October 1987).

31. C. Baas, M. Barnier, J. P. Beylot, P. Martel, and F. Merchie, "Progress Report on LEU Fuel Testing in CEA Reactors," Proc. 1986 Int. Mtg. on Reduced Enrichment for Research and Test Reactors, Gatlinburg, Tennessee, November 3-6, 1986, Argonne National Laboratory Report ANL/RERTR/TM-9, in press.

32. F. Merchie, CEN-G, personal communication (July 1987).

33. J. M. Beeston, R. R. Hobbins, G. W. Gibson, and W. C. Francis, "Development and Irradiation Performance of Uranium Aluminide Fuels in Test Reactors," Nucl. Tech. 49, 136-149 (June 1980).

34. G. L. Hofman, G. L. Copeland, and J. E. Sanecki, "Microscopic Investigation into the Irradiation Behavior of U_3O_8-Al Dispersion Fuel," Nucl. Tech. 72, 338-344 (1986).

35. A. E. Richt, R. W. Knight, and G. M. Adamson, Jr., "Postirradiation Examination and Evaluation of the Performance of HFIR Fuel Elements," Oak Ridge National Laboratory Report ORNL-4714 (December 1968).

36. D. Stahl, "Fuels for Research and Test Reactors, Status Review: July 1982," Argonne National Laboratory Report ANL-83-5, pp. 37-39 (December 1982).

37. R. E. Woodley, "The Release of Fission Products from Irradiated SRP Fuels at Elevated Temperature," Hanford Engineering Development Laboratory Report HEDL-7598 (June 1986).

38. T. Shibata, T. Tamai, M. Hayashi, J. C. Posey, and J. L. Snelgrove, "Release of Fission Products from Irradiated Aluminide Fuel at High Temperatures," Nucl. Sci. and Eng. 87, 405-417 (1984).

39. J. C. Posey, "Release of Fission Products from Miniature Fuel Plates at Elevated Temperatures," Proc. Int. Mtg. on Research and Test Reactor Core Conversions from HEU to LEU Fuels, Argonne, Illinois, November 8-10, 1982, Argonne National Laboratory Report ANL/RERTR/TM-4 (CONF-821155), pp. 117-133 (September 1983).

40. G. W. Parker, G. E. Creek, C. J. Barton, W. J. Martin, and R. A. Lorenz, "Out-of-Pile Studies of Fission-Product Release from Overheated Reactor Fuels at ORNL, 1955-1965," Oak Ridge National Laboratory Report ORNL-3981 (July 1967).

41. G. C. Rodrigues and A. P. Gouge, "Reprocessing RERTR Silicide Fuels," Savannah River Laboratory Report DP-1657 (May 1983).

42. U.S. Department of Energy, "Receipt and Financial Settlement Provisions for Nuclear Research Reactor Fuels," Federal Register 51(32), 5754-5756 (February 18, 1986) and Federal Register 51(42), 7487 (March 4, 1986).

DISTRIBUTION FOR ANL/RERTR/TM-11

Internal:

A. Schriesheim
C. E. Till
P. I. Amundson
L. Burris
D. W. Cissel
L. G. LeSage
R. A. Lewis
J. F. Marchaterre
R. J. Teunis
D. C. Wade
R. W. Weeks
A. Travelli (144)
J. L. Snelgrove (2)
R. F. Domagala (2)
G. L. Hofman (2)
F. J. Karasek
L. A. Neimark
D. R. Schmitt
H. R. Thresh
T. C. Wiencek (2)
ANL Contract File
ANL Patent Department
ANL Libraries (2)
TIS Files (5)

External:

DOE-TIC, for distribution per UC-83 (41)

Manager, Chicago Operations Office, DOE

Director, Technology Management Div., DOE-CH

J. P. Colton, ACDA
D. E. Bailey, DOE-NE
L. S. Rubenstein, NRC (2)
D. Stahl, SAI

ORNL:

E. D. Clemmer
G. L. Copeland (2)
R. W. Hobbs (2)
S. S. Hurt
R. W. Knight
D. L. Selby
R. L. Senn (2)
L. G. Shrader
J. H. Swanks
C. D. West

INEL:

K. R. Brown
R. E. Carter
C. H. Cooper
R. R. Hobbins
J. A. Lake
L. K. Seymour

C. Benjamin Alcock, The University of Toronto
Paul C. Shewmon, Ohio State University

Applied Physics Division Review Committee:

Paul W. Dickson, Jr., EG&G Idaho, Inc.
E. Linn Draper, Gulf State Utilities
Michael J. Driscoll, Massachusetts Institute of Technology
Robert L. Hellens, West Simsbury, Connecticut
William E. Kastenberg, University of California-L.A.
Daniel A. Meneley, University of New Brunswick
Warren F. Miller, Los Alamos National Laboratory